



INSTITUT FÜR
ENERGIETECHNIK UND
THERMODYNAMIK

Institute for Energy Systems and Thermodynamics

Diplomarbeit

Reduction approaches in thermal building simulations for an industrial food production facility

ausgeführt zum Zwecke der Erlangung des akademischen Grades eines
Diplom-Ingenieurs unter der Leitung von

Ao. Univ. Prof. Dipl.-Ing. Dr. techn. Karl PONWEISER

und

Projektass. Dipl.-Ing. Peter SMOLEK, BSc

Projektass. Dipl.-Ing. Ines LEOBNER

Institut für Energietechnik und Thermodynamik

eingereicht an der Technischen Universität Wien

Fakultät für Maschinenwesen und Betriebswissenschaften

von

Michael STARKMANN, BSc

e0927755

Kirchberggasse 37 / 2

1070 Wien

Wien, am 15.10.2015

Michael Starkmann

Eidesstattliche Erklärung

Ich erkläre an Eides statt, dass ich meine Diplomarbeit nach den anerkannten Grundsätzen für wissenschaftliche Abhandlungen selbstständig ausgeführt habe und alle verwendeten Hilfsmittel, insbesondere die zugrunde gelegte Literatur genannt habe.

Weiters erkläre ich, dass ich dieses Diplomarbeitsthema bisher weder im In- noch im Ausland (einer Beurteilerin/einem Beurteiler zur Begutachtung) in irgendeiner Form als Prüfungsarbeit vorgelegt habe und dass diese Arbeit mit der vom Begutachter beurteilten Arbeit übereinstimmt.

Wien, am 15.10.2015

Starkmann Michael

Abstract

New technologies and increased requirements in thermal building simulations, especially in terms of simplicity and computation time, boost the development of simplified building simulations. A simplified thermal building simulation model based on the resistance capacitance method is introduced. The model consists of transient energy balance equations for the zone air, walls and the wall surfaces. The thermal capacity of walls is taken into account, which makes the model suitable for a wide range of applications. The introduced thermal building model is implemented in the equation-based Modelica language.

With the help of this model an industrial food production facility is analyzed in terms of heating and cooling demand as well as indoor air temperature. The results are compared to a detailed EnergyPlus simulation and the accuracy and computation time are discussed.

The modular concept of the proposed model allows to easily simplify it. Various simplifications were conducted in order to show the influence of certain parameters on the model. Especially the simplified convection model leads to a significantly reduced computation time while maintaining a similar accuracy as the more complex convection model. This makes it particularly suitable for the use in the early design phase.

Kurzfassung

Neue Entwicklungen und erhöhte Anforderungen an thermische Gebäudesimulationen, speziell in Bezug auf Einfachheit des Modells und notwendiger Simulationszeit, steigern den Bedarf an vereinfachten thermischen Gebäudesimulationen. Basierend auf der Widerstand-Kapazitäts (RC) Methode wurde ein Simulationsmodell erstellt. Dieses besteht aus instationären Energiebilanzgleichungen für die Raumluft, die Wände und die Wandoberflächen. Die Wärmespeicherkapazität der Wände ist ein wichtiger Bestandteil des Modells und es kann daher vielseitig angewandt werden. Das vorgestellte Simulationsmodell wurde in der gleichungsbasierten Modelica Sprache implementiert.

Der Heiz- und Kühlbedarf sowie die Raumtemperatur einer industriellen Lebensmittelproduktionsstätte wurden mit diesem Model simuliert. Verglichen mit einer detaillierten EnergyPlus-Simulation zeigt das vorgestellte Modell einen guten Kompromiss aus Genauigkeit und benötigter Simulationszeit.

Der modulare Aufbau des Modelles erlaubt dieses weiter zu vereinfachen. Um den Einfluss verschiedener Parameter auf das Modell zu zeigen wurden mehrere Vereinfachungen durchgeführt. Ein simpleres Konvektionsmodell reduziert die Simulationszeit signifikant, bei einer ähnlich hohen Genauigkeit der Simulationsergebnisse im Vergleich zum genauen Konvektionsmodell. Daher eignet sich das einfache Konvektionsmodell sehr gut für die Anwendung in der frühen Designphase eines Gebäudes.

Table of Contents

1	Introduction	1
2	Thermal building simulation	3
2.1	Use	3
2.2	History	3
2.3	Overview of methods	4
2.3.1	Physical models	4
2.3.2	Statistical methods	6
2.3.3	Hybrid models	7
2.4	Trends	8
3	Selected approaches and software	9
3.1	Resistance capacitance models	9
3.2	Modelica	11
3.3	Differences between EnergyPlus and the proposed model	11
3.3.1	Initial values	11
3.3.2	Wall model	12
3.3.3	Solar radiation	13
4	Building	15
5	Dymola model	17
5.1	Energy balance for the internal air volume	17
5.2	Building envelope	18
5.2.1	Energy balance for walls and ceilings	19
5.2.2	Energy balance for floors	20
5.3	Convection	21
5.3.1	Convective heat transfer coefficients	22
5.4	Windows and doors	23
5.5	Infiltration	23
5.6	Solar radiation on surfaces	23
5.6.1	Reckoning of time	23
5.6.2	Solar angles	24
5.6.3	Incidence angle	26
5.6.4	Solar radiation on surfaces	28
5.7	Solar contributions	30
5.7.1	Solar radiation on opaque walls	30
5.7.2	Solar radiation through windows	30
5.8	Initialization of the model	31
6	Comparison of the Dymola model to the reference simulation	35
6.1	Detailed convection model	35
7	Model simplifications	39
7.1	Simple convection model	39
7.2	Constant convection coefficients	41
7.3	Simple floor model	44
7.4	Lumped walls	45
7.5	Solar radiation	50

7.6	Neglected thermal capacity of walls	52
7.7	Minimal model	54
7.8	Computation time	56
7.9	Verdict	58
8	Conclusion and outlook	59
A	Modelica code for the detailed convection model	1

Nomenclature

Roman letters

A	area (m^2)
AST	apparent solar time (h)
a	thermal diffusivity ($\text{m}^2 \text{s}^{-1}$)
a, b	forced convection coefficient, or
a, b	limited incidence angles for Perez model
B	function dependent on the day of the year (d)
C	thermal capacitance (J K^{-1})
C_{eff}	effective thermal capacitance (J K^{-1})
C_t	natural convection coefficient ($\text{W m}^{-2} \text{K}^{-4/3}$)
c	specific heat ($\text{J kg}^{-1} \text{K}^{-1}$)
d	thickness (m)
DS	daylight saving (either 0 or 1h)
ET	equation of time (min)
F_1, F_2	brightening coefficient
$F_{11}-F_{23}$	constants for calculation of the brightening coefficients
f	factor of shading
$\dot{H}C$	sensible heating or cooling power (W)
h	convective heat transfer coefficient ($\text{W m}^{-2} \text{K}^{-1}$), or
h	hour angle ($^\circ$)
h_{irr}	radiative heat transfer coefficient ($\text{W m}^{-2} \text{K}^{-1}$)
h_{tot}	total heat transfer coefficient ($\text{W m}^{-2} \text{K}^{-1}$)
I_i	global solar radiation (W m^{-2})
I_0	extraterrestrial irradiance (W m^{-2})
\dot{L}	internal gains (W)
LL	local longitude ($^\circ$)
LST	local standard time (h)
m	relative optical air mass
MBE	mean bias error
N	day of the year (d)
n	infiltration rate (h^{-1})
Q, \dot{q}	heat flux (W)
R	thermal resistance (K W^{-1})
$RMSE$	root mean square error
s	wall layer thickness (m)
SL	standard longitude ($^\circ$)
T	temperature ($^\circ\text{C}$)
T_{ext}	equivalent exterior temperature ($^\circ\text{C}$)
U	transmittance ($\text{W m}^{-2} \text{K}^{-1}$)
UA_e	thermal conductance to external environment (W K^{-1})
V	volume (m^3)
v_{ws}	windspeed (m s^{-1})
z	solar azimuth angle ($^\circ$)
Z_s	surface azimuth angle ($^\circ$)

Greek letters

α	solar altitude angle ($^{\circ}$), or
α	solar absorptance
β	surface tilt angle ($^{\circ}$)
Δ	sky brightness
δ	solar declination ($^{\circ}$)
ϵ	emissivity, or
ϵ	sky clearness
θ	solar incidence angle ($^{\circ}$)
κ	constant for calculation of sky ($\kappa = 1.041$)
λ	thermal conductivity ($\text{W m}^{-1} \text{K}^{-1}$)
ξ_r	tilt solar redirected radiation factor
ρ	density (kg m^{-3}), or
ρ	ground reflectivity
σ	Stefan Boltzmann constant ($\text{W m}^{-2} \text{K}^{-4}$)
τ	glass transmission coefficient
Φ	solar zenith angle ($^{\circ}$)

Subscripts

<i>air</i>	air
<i>amb</i>	ambient
<i>b</i>	beam
<i>co</i>	convection
<i>d</i>	direct
<i>e</i>	exterior
<i>f</i>	floor
<i>h</i>	horizontal
<i>i</i>	interior, or
<i>i</i>	index for i^{th} wall
<i>inf</i>	infiltration
<i>j</i>	index for j^{th} floor
<i>k</i>	index for various purposes
<i>win</i>	windows

1 Introduction

Households and commercial buildings consume about one third of the global final energy demand and are accountable for 30% of CO₂ emissions [1]. Furthermore the energy demand of buildings is still on the rise. Designing and building energy efficient buildings is the key to lower the global final energy demand. However, thermal building simulation is a complex task due to the various thermal phenomena involved. Some of them are especially difficult to model accurately. Figure 1 shows the typically involved thermal phenomena. A plethora of thermal building simulation programs is available. The energy demand of a building is roughly determined in the early planning phase, but not all physical properties are settled in this early stage. Therefore building simulations are done when the design phase is completed, allowing one to examine the energy demand of a building. The drawback of this procedure is that one cannot compare different building designs to each other. Also detailed thermal building simulations require a high skill level and a lot of man-hours to conduct them. Fast and accurate simple building simulation models can overcome these drawbacks and help to make ideal design decisions already in the earliest design phase. Furthermore new technologies in energy efficient buildings, especially phase change materials and free cooling, are only applicable in transient simulations taking the thermal inertia into account [2]. The following work presents a simplified building simulation model - based on electrical analogy - implemented in Modelica. An industrial food production facility is analyzed and the results are compared to a detailed simulation. The proposed model shows a very good accuracy compared to the detailed building simulation (EnergyPlus). In addition this model can be simplified further in order to lower computation time or amount of necessary input parameters.

This thesis is divided into several chapters. First, an introduction to thermal building simulation is given. Containing the field of application and utilization of building simulation, a short history of building simulation methods and tools, a detailed overview of building simulation methods and an outlook of future trends in this discipline. The next chapter goes into detail about the nodal approach, which is the basis for most building simulation software as well as simplified models. A description of thermal resistance capacitance (RC) models is given along with a critical examination of this method. This chapter also lists the differences between the proposed model and the detailed EnergyPlus simulation. Chapter 4 presents the analyzed industrial food production facility and lists the analyzed thermal zones. Due to time constraints only a few zones could be analyzed. Therefore four different zones were chosen in order to boost the understanding of the proposed model and get more vital insight. Chapter 5 presents the proposed model in detail. This model contains energy balances for the zone air, wall and wall surfaces. The main focus lies on the wall model as it is relevant for the complexity, accuracy and computation time of the model. The convection model is presented in detail because it also has a crucial impact on the proposed model. Chapter 6 compares the results of the proposed model to a detailed EnergyPlus simulation. The heating and cooling demand over a year is shown for all four zones as well as indoor air-temperatures. Also the deviation of heating- and cooling demand and overall energy demand is listed, as well as statistical characteristics factors. As the proposed model shows a good agreement between accuracy and simulation time other applications de-

mand lower to very low computation time or fewer input parameters. Therefore various simplifications of the proposed model are introduced in chapter 7. These simplifications are also analyzed in terms of accuracy and speed. At the end of this chapter a summary of these simplifications is given with recommendations regarding their usability. The last chapter is the conclusion and provides a short outlook for further possibilities of the proposed model.

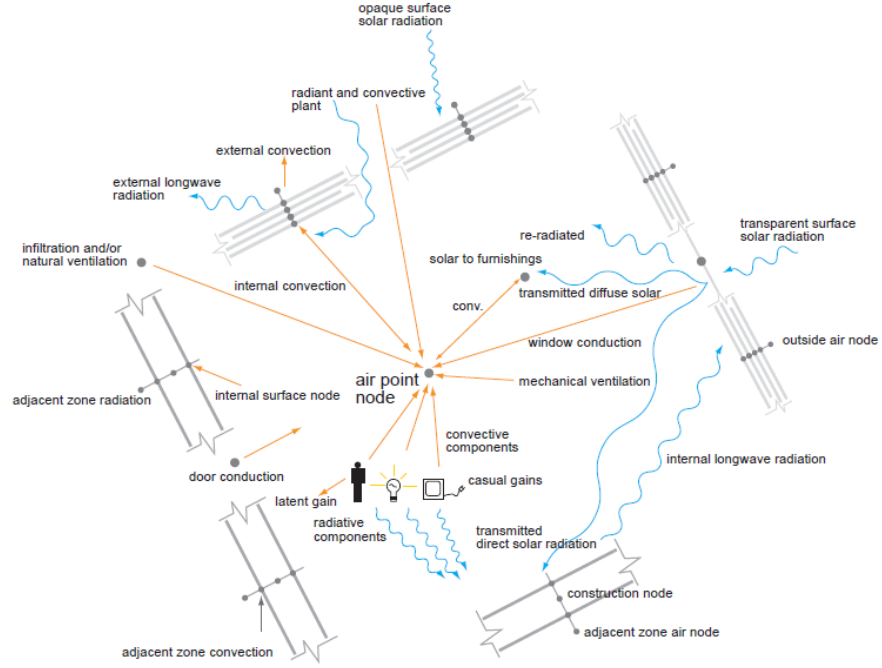


Figure 1: Thermal phenomena in building simulations [3, p.6].

2 Thermal building simulation

Buildings have a major share in world wide energy consumption. Facing future obstacles in energy supply and prices as well as pollution through resourcing of energy, energy efficient buildings are a key to lower the energy demand and preserve our environment. Thermal building simulations are used for the design, prediction and optimization of a buildings thermal performance. This chapter gives insight into the benefits and history of building simulations, a detailed overview of simulation methods and future trends.

2.1 Use

Thermal building simulations are used for a plethora of tasks, ranging from the evaluation of design alternatives, compliance with energy standards and regulations, optimization of energy demand or thermal comfort and many more. The motivation for conducting building simulations are:

- In the next decades most people will live in buildings already built. Buildings are replaced at a slow pace and have a very long life-span. Therefore energy efficiency is crucial for new-built buildings.
- The energy demand of a building is roughly determined at the early design stage with little room for retrofitting the building due to high modification costs (see figure 2 on page 4).
- Energy prices are exposed to fluctuations.
- Indoor comfort and air-quality become more and more important. Well designed buildings help to establish a high level of comfort and a healthy indoor environment.
- Calculate the payback period of investments in energy efficiency of new buildings.
- “Simulation is the only way to allow the designer to explore the complex relationships between environment and building’s form, fabric, services and control.” [4, p.638]

2.2 History

The widespread use of thermal building simulations began in the 1970s in the research community and in the 1990s it stretched out to professional practice. The time delay between the use in research to practical application was caused by the required high level of know-how and the costs connected to it. Building simulations have their roots in the 1960s. Before that time HVAC calculations were done by hand and focused on the sizing of the HVAC-equipment, which often resulted in over-sized equipment and high heating and cooling loads. However the 1960s mark the time of the first use of computers for thermal building simulations. Later, in the 1970s, the simulation programs were refined and lead to the birth of DOE-2 (now EnergyPlus) and TRNSYS, which are still popular today. The reason for the rapid evolution of building simulation software was the oil embargo of 1973. The passing of the oil embargo lowered the incentives

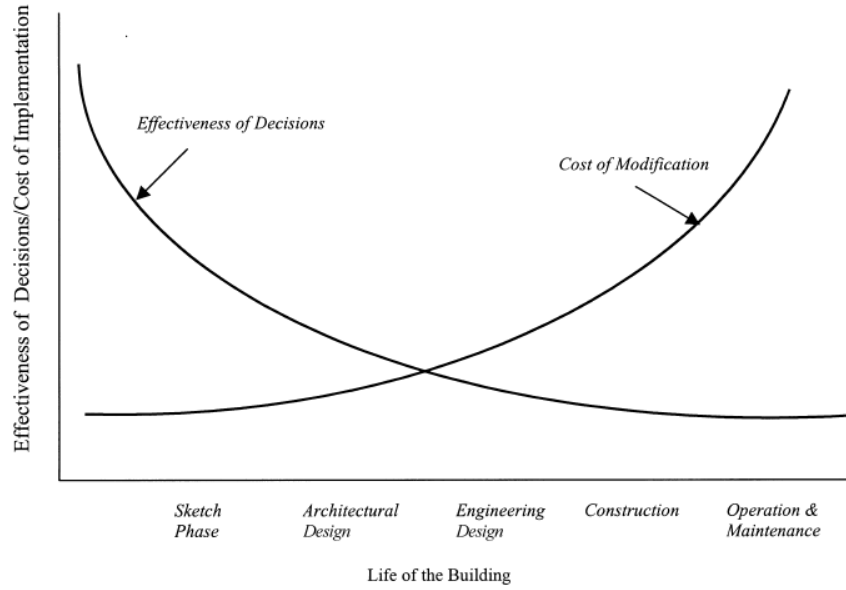


Figure 2: Decision costs and their impact on the performance of buildings [5, p.422].

for building simulation, however advancements in personal computing power renewed the interest [6]. The 1980s were predominated by the refinement of programs. The 1990s marked the transition from research to professional use with more powerful and affordable computers and easier to use programs. Also building information modeling (BIM) programs were coupled with building energy modeling (BEM) programs. After the millennium the collaboration of BIM and BEM programs tightened and is still ongoing. Today the need for green buildings and tighter regulations made the use of thermal building simulations necessary. Especially simple and fast simulations help to estimate the building's energy demand in early design stages.

2.3 Overview of methods

The ongoing increase of processing power over the last decades made it possible to evolve from manually calculated heating and cooling loads to complex thermodynamic simulations. Today a plethora of different simulation programs is available, each with its own advantages and disadvantages. However they can be generally classified into physical models (based on solving the equations describing the physical behavior of the heat transfer), statistical methods and hybrid models (coupling of physical models and statistical methods).

2.3.1 Physical models

Physical models are often referred to as engineering methods or white box models. All physical models are based on solving equations which describe the

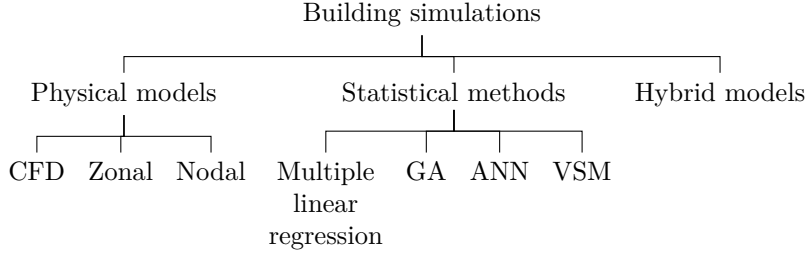


Figure 3: Overview of thermodynamic building simulation methods.

physical behavior of the heat transfer [7]. Based on the energy conservation law follows:

$$Q_{int} + Q_{source} = Q_{out} + Q_{stock} \quad (1)$$

Q_{int} and Q_{out} represent the incoming respectively the outgoing heat flux. Q_{source} the heat flux of a possible heat source and Q_{stock} a stored heat flux.

Computational Fluid Dynamics Approach (CFD)

The CFD approach is the most sophisticated of the physical models. The CFD model requires an accurate building model and divides each zone in a large amount of control volumes. This control volumes can either have a homogeneous or heterogeneous global mesh [7]. Based on this model the software solves the Navier-Stokes equations.

The biggest advantage is that detailed airflows (but not limited to airflows alone) can be examined. Also it is possible to locally enhance the amount of control volumes and therefore get more accurate results in this area. The biggest drawback is the huge computation time needed. However the CFD method can be coupled with simpler methods in order to gain shorter computation times while still achieving feasible results.

Zonal Approach

The zonal approach divides each zone into several cells. It is basically a simplification of the CFD approach. Therefore the zonal approach is not as viable as the CFD approach to study the detailed description of the flow field. However, for simpler indoor thermal comfort and ventilation simulations the zonal approach is sufficient. The main advantage is the considerably lower computation time compared to the CFD method.

Nodal Approach

The nodal approach¹ is again a simplification of the zonal approach. It is therefore the simplest of the presented physical models. In the nodal approach every building zone is modeled as a homogeneous volume characterized by uniform state variables (temperature, pressure, etc.) [7].

The nodal approach can furthermore be divided into two different methods (see figure 4). The first method is based on solving the transfer functions for

¹The nodal approach is also known as multizone approach.

each node. Most software uses this method, among them are for example EnergyPlus and TrnSys. The finite difference method uses an electrical analogy in order to shorten computation time. This is reached via linearization of the equations. The even further reduced computation time makes this model suitable for monitoring and control applications.

The big advantage of the nodal approach is that it is a well adapted tool for the estimation of energy consumption. Especially the low computation time allows simulations on large time scales. However, modelling of thermal comfort, air quality and impact of loads on close environment are difficult to model and should be done with the zonal or CFD approach.

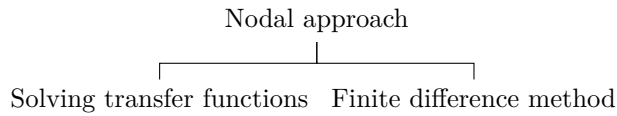


Figure 4: Overview of nodal approach methods.

2.3.2 Statistical methods

Contrary to the physical models the statistical methods do not require any of the physical equations (Navier-Stokes equations, transfer functions). Also they require less data of the physical system. Their inputs are samples of training data. The statistical methods use this data to describe the behavior of a system. In most cases the statistical methods correlate the energy consumption or energy index with influencing variables (e.g. weather variables, climate index, etc.). The biggest advantage of statistical methods is that they do not need a detailed building description. However the amount and quality of the training data is crucial for the quality of the results. An overview of statistical methods is given in figure 3. Note that not all statistical methods require learning or training algorithms [8].

Multiple linear regression or conditional demand analysis (CDA)

The CDA method uses a linear combination of input variables (e.g. outdoor temperature, solar radiation, etc.) plus an error term to predict an output variable (e.g. indoor temperature). It is mainly used for prediction, forecasting and data mining [7]. The biggest advantage of CDA is that it is easy to use (no tuning of parameters as in other statistical methods) and delivers good results in terms of accuracy. However there are several drawbacks. First, the CDA is not able to treat non-linear problems. Second, it is difficult to manage the multicollinearity inside the prediction results [7]. And last, large quantities of data are required in order to achieve proper results.

Genetic algorithm (GA)

GAs are part of the evolutionary algorithms. The evolutionary algorithms are inspired by Darwin's process of natural selection. They are used for solving a wide variety of optimization and search problems. In contrast to the CDA the genetic algorithm method is able to treat linear and non-linear problems. The user has to impose the form of the equation (e.g. linear, quadratic,

exponential)[7]. The GA delivers several final solutions, which are not necessarily optimal solutions. Drawbacks are that the user has to choose the most plausible solution, however he cannot be sure that his chosen solution is the best solution. Also the adjustment of the algorithm is done via testing different combinations which prolongs the already high computation time. Nevertheless the GA is used for simple predictions of energy demand and optimization.

Artificial neural network (ANN)

“ANNs are the most widely used artificial intelligence models in the application of building energy prediction.” [9, p.3588] The ANN is a non-linear statistical tool inspired by the function of the central nervous system. It is good at solving non-linear problems and overcomes the shortcomings of the CDA and GA. One of the main advantages of the ANN method is that it is able to identify the relationship between different variables but does not rely on assumptions and postulates for doing that [7]. The ANN method needs a relevant and complete database and also a large amount of training data (e.g. on-site measurements, bills, simulations, etc.). Another drawback is the large number of undetermined parameters and the lack of interpretability of the system.

Support vector machine (SVM)

The SVM method tries to find the optimal generalization of the model. It is based on the structural risk minimization principle [7]. The user has to impose a kernel function (e.g. linear, polynomial, radial basis function). Advantageous is the fact that SVM requires fewer parameters for tuning compared to GA and ANN. The biggest advantage is that SVM supports a heterogeneous database. That means that variables can have different amounts of information and even missing data can be handled.

2.3.3 Hybrid models

Hybrid models (grey box models) are a combination of physical and statistical methods in order to overcome the hindrances of them. Physical models require all building characteristics to be known (which is very difficult if examining existing buildings). Furthermore it is difficult to model all physical phenomena accurately (e.g. natural ventilation, ...). Statistical models, on the other hand, require a huge amount of data and are limited in terms of physical interpretability. The big advantage of hybrid models is that statistical tools are used in order to find missing building characteristics. To date three different strategies are used by the scientific community. First, using machine learning as physical parameters estimator. Second, use statistics in order to implement a learning model characterizing the building behavior based on a physical approach. Third, use statistics in areas where physical models are not efficient (computation time) and/or accurate enough [7]. Given the novelty of hybrid models there is still room for new strategies to emerge. Hybrid models are primarily used for parameter estimation and monitoring (HVAC control). The biggest disadvantage is the computation time, however hybrid models are not slow by principle.

2.4 Trends

The need to reduce software cost and development time as well as the integration of tools in a coherent workflow are the main drivers of the future development of building simulation tools. Equation-based object-oriented models are easy to implement and reuse which reduces software costs and development time significantly [10]. Over the last years the number of research projects working with object-oriented tools (e.g. Modelica) increased constantly and will still be on the rise.

Another big trend for the future is integrated building design systems (IBDS). Different building software tools for different purposes are included and exchange data through a standardized database [6]. One step ahead are building simulations which are generated by the building information model. Overall different simulations for buildings (e.g. construction costs, control schemes, thermal, maintenance costs, etc.) will complement each other and exchange data.

Building simulations for early design stages will become more and more important. The energy demand is roughly determined by choices in the early design stage with little potential of significant improvements after that phase. Figure 2 on page 4 shows the trend of modification costs of buildings over its lifespan. Clearly simple tools are needed which calculate the energy demand with little available information in early design stages in order to achieve energy efficient buildings.

3 Selected approaches and software

The multizone or nodal approach is considered the simplest physical model for building simulations (see chapter 2.3.1). They can be solved by extensive software packages like Energy Plus and TRNSYS which use a flat representation of the building energy system. However such software tools mix physical models with numerical solution algorithms [11]. Additionally the user has no control over the numerical solution algorithms. Furthermore these software tools do not allow the user to define initial values or equations. Another drawback is that these software programs do not really allow the user to conduct multiple simulation runs in order to find optimal values or controlling strategies. Last but not least, new program extensions for existing simulation suits require programming knowledge and are complicated to implement. Equation-based object-oriented modeling languages like Modelica and Matlab on the other hand can overcome most of the stated drawbacks. Especially the shorter model development time and flexibility is a huge advantage of equation-based object-orientated modeling languages.

3.1 Resistance capacitance models

Thermal resistance capacitance (RC) models are basically the simplest models used for thermal building simulations. The heat equation without inner heat sources and temperature independent thermal conductivity in Cartesian coordinates:

$$\frac{dT}{dt} = a \left(\frac{d^2T}{dx^2} + \frac{d^2T}{dy^2} + \frac{d^2T}{dz^2} \right) \quad (2)$$

is a parabolic partial differential equation. This equation can numerically be solved by the finite difference method. The RC network method is based on the finite difference method and is physically motivated by the analogy of thermal and electrical quantities. The analogy of thermal and electrical systems allows the representation of thermal properties through a network of electrical components. The thermal problem is translated into an electrical problem which can be solved by Kirchhoff's current law. Table 1 lists thermal quantities represented by electrical quantities.

The RC network method discretizes the heat equation into spatial components. A wall layer is considered with the thickness Δx and thermal resistance R (see figure 5). The conduction equation is written as [12, p.1018]:

$$\frac{T(x + \frac{\Delta x}{2}, t) - T(x, t)}{\frac{R}{2}} + \frac{T(x - \frac{\Delta x}{2}, t) - T(x, t)}{\frac{R}{2}} \approx C \frac{dT(x, t)}{dt} \quad (3)$$

Limitations and assumptions

All nodal models are based on the assumption of a uniform zone air-temperature. For small zones this assumption often holds, however huge zones with high ceiling-height (e.g. the zone *production hall*, see figure 7 and 8) probably do not have a well mixed indoor air-temperature.

In general research on RC-models focused on model order and lumping parameters, however there is no research on what input-parameters are crucial and how they should be implemented in the model [13].

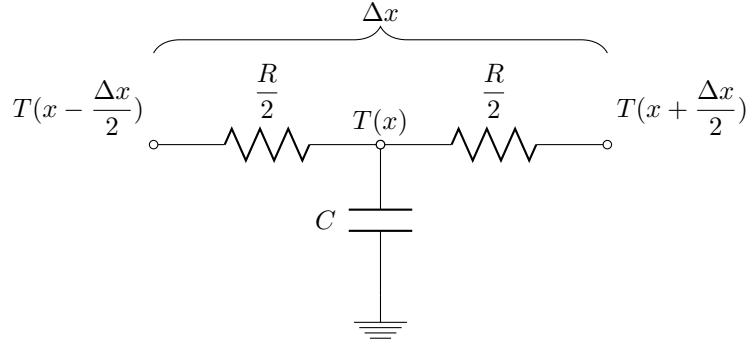


Figure 5: Electrical analogy of conduction through a wall layer.

Table 1: Thermal-electric analogy [14, p.5].

Electrical Analogy			Thermal Analogy		
Quantity	Symbol	Unit	Quantity	Symbol	Unit
Voltage	U	V	Temperature	T	$^{\circ}C$
Current	I	A	Heat Transfer Rate	\dot{Q}	W
Electrical Resistance	R	Ω	Thermal Resistance	R	$^{\circ}C W^{-1}$
Electrical Capacitance	C	F	Thermal Capacitance	C	$J ^{\circ}C^{-1}$
Ohm's Law	$I = \frac{\Delta U}{R}$		Steady Heat Conduction	$\dot{Q} = \frac{\Delta T}{R}$	
Current through Capacitor	$I = C \frac{dU}{dt}$		Thermal Capacitance Heat Flow Rate	$\dot{Q} = C \frac{dT}{dt}$	
Kirchhoff's Current Law			Heat Balance		

As the internal vapor generation rate is supposed to be rather small most RC-models deal only with temperature and not with temperature and air humidity [15].

3.2 Modelica

The proposed model is implemented with Modelica. Modelica is an equation-based object-oriented modeling language, first released in 1997. It has an extensive standard library which helps to quickly set up models. Traditional building simulation software lacks the flexibility and expandability of Modelica models. As a result Modelica is used for a plethora of applications which can hardly be examined by traditional building simulation software. Especially the faster development time and ability to reuse, adapt and extend the model makes Modelica suitable for the proposed examination approaches [11]. Another advantage of Modelica is that the user has full control over numerical solution algorithms. However the biggest advantage of Modelica is that models can be described acausal, meaning that the model is described by a set of equations rather than assignments. Therefore Modelica allows to concentrate on the models formulation rather than handling confusing GUIs (building simulation programs) or low level programming necessities. The Modelica code of the presented model is shown in appendix A. As Modelica is only a modeling language, a modeling and simulation environment is necessary. For this study the commercial modeling and simulation environment Dymola (DYnamic MOdeling LAnguage) was used. Dymola offers efficient and stable solvers and multiple useful visualization tools. Other implementations of the Modelica language are e.g. OpenModelica (open-source) and various others.

3.3 Differences between EnergyPlus and the proposed model

Although both, the reference EnergyPlus simulation and the proposed equation-based Modelica model, are based on the multizone approach there are differences between the models. The differences in the initial value problem, wall model, convection, solar radiation calculation and windows are discussed.

3.3.1 Initial values

The EnergyPlus model and the proposed model need initial values. These initial values are crucial as a sloppy initialization distorts the simulation results in the first few days or weeks. Especially short term simulations suffer from wrong initial values. To circumvent this issue EnergyPlus uses warmup days. A number of days are simulated before the actual simulation starts until the temperatures and heat fluxes on the first day converge. [16] lists the convergence criteria. The proposed model uses an estimation of the wall temperatures based on the thermal resistances of the wall (see chapter 5.8). Additionally a method using a dummy simulation period before the proper simulation is presented.

3.3.2 Wall model

The biggest difference between EnergyPlus and the proposed model is the wall model. EnergyPlus uses the state space method for calculating the conduction transfer function (CTF). The CTF method relates the heat flux at a surface linearly to the current and previous wall surface temperatures and previous heat fluxes. This leads to a fast model with a simple linear equation with constant coefficients. No inside wall temperatures have to be calculated or saved (only the wall surface temperatures). The proposed model on the other hand uses the finite difference thermal network approach in which a wall is discretized into two or more sub-layers. Contrary to CTF, this method is capable of modeling non-linear effects and temperature dependent behavior (e.g. for phase-change materials). Figure 6 shows the EnergyPlus wall model in electrical analogy. Compared to the proposed model (see figure 10 on page 19) we see two main differences:

- The proposed model has one capacitance in the middle of the wall (therefore a wall temperature in the middle of the wall is also calculated) while EnergyPlus discretizes the wall into two capacitances sitting on the wall's interior and exterior surface. Therefore the EnergyPlus model has a higher order (2-nodes) than the proposed model (1-node).
- EnergyPlus has one conductive resistance for the wall while the proposed model splits the conductive resistances into two separate resistances.

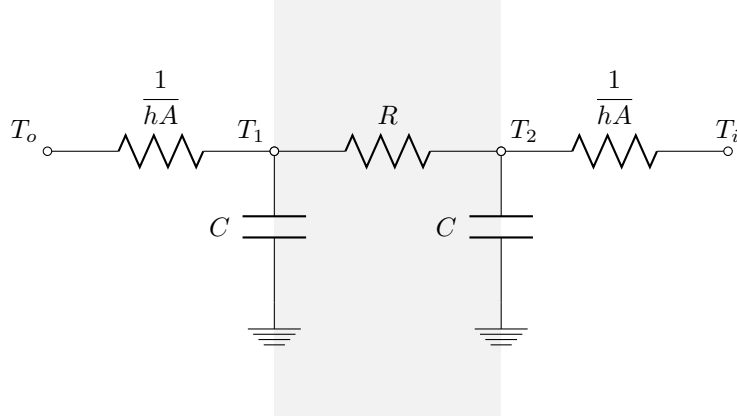


Figure 6: Wall model in EnergyPlus.

In general the higher order (1R2C) EnergyPlus model will yield better results than the simpler proposed wall-model (2R1C). However higher order models are more computation intensive (1 differential equation for each node). The comparison of the proposed model to the EnergyPlus simulation (chapter 6.1) shows that the simpler 2R1C model reaches comparable results to the 1R2C model.

Exterior wall surface heat balance

The EnergyPlus model takes long wave radiation into account while the presented model does not. The influence of longwave radiation was neglected in

the presented Dymola model because longwave radiation has a minor impact on the energy balance of the exterior wall surfaces. For the energy balance of interior wall surfaces longwave radiation has a considerable influence, however longwave radiation is difficult to take into account for complex zone geometries and would have prolonged computation times significantly. EnergyPlus has several different convection algorithms implemented. For the exterior convection coefficient the DOE-2 algorithm² was used.

Interior wall surface heat balance

The EnergyPlus interior wall surface model is more complex than the exterior wall surface model. It has an algorithm for determining longwave radiant exchange flux between surfaces and shortwave radiation flux to a wall's surface. The provided EnergyPlus simulation uses the TARP algorithm³ in order to calculate the convection coefficient while the presented Dymola model uses an adjusted MoWiTT algorithm (see chapter 5.3.1).

Floor model

EnergyPlus uses a complex model for the calculation of heat fluxes between the ground and the floor which requires constant ground temperatures for a full month. A detailed reference of the ground model is found in [17]. The provided EnergyPlus simulation used a ground temperature of 17°C for every single month, therefore the proposed Dymola model used the same ground temperature.

3.3.3 Solar radiation

The calculation of solar radiation is the same for the presented model and the EnergyPlus simulation, both use the Perez diffuse sky model. The only difference is that EnergyPlus has higher precision constants F_{11} – F_{23} (4 additional digits). The used (lower-precision) constants are listed in table 5 on page 30. More information on the calculation of solar radiation is found in chapter 5.6.

Shading

The analyzed building's windows are shaded by fixed fins. The presented model does not take the reduced solar radiation through shading into account. The effect of shading was neglected because the goal was to implement a very basic and fast model. Note that the reduced solar radiation has a distinct influence on the heating and cooling demand, especially in the summer period. However it is possible to add shading to the proposed Dymola model.

Windows

The EnergyPlus window model estimates solar properties of the window based

²The DOE-2 algorithm is an algorithm for the calculation of the convection coefficient. It is based on a combination of two different convection models.

³The TARP algorithm is an algorithm for the calculation of the convection coefficient. It is based on a term for natural and a term for forced convection.

on the u-value⁴ and SHGC⁵ of the window. The algorithm is shown in [16]. The presented model uses a far more simpler window model. However, both models do not take the thermal capacity of windows into account.

⁴The u-value is the heat transfer coefficient of a building element. It is the inverse of the thermal resistance R.

⁵The solar heat gain coefficient is the fraction of incident solar radiation that enters through the window as heat gain.

4 Building

An industrial food production facility is analyzed in terms of heating and cooling demand as well as indoor temperatures. The analyzed building is located in Tyrol (Austria) and the evaluation of its energy demand is part of the project Balanced Manufacturing (BaMa). The project started in 2014 and aims at increasing the overall energy efficiency of production facilities by simulation and optimization of the production system, building, energy supply and logistics.⁶ The detailed EnergyPlus simulation of the analyzed facility was provided by DI Georgios Gourlis from the Institute of Interdisciplinary Construction Process Management. It will be tested against the proposed Dymola model.

The building itself is 3-stories high and consists of 3 blocks. As the focus of the simulation lies on the bakery and the pastry shop the right-hand side of the facility is more detailed than the left-hand side (see figure 7). The block on the right-hand side of figure 7 contains departments for incoming and outgoing goods, storage, a huge production hall containing the bakery, a pastry shop partly above the bakery, energy-system equipment and offices. The block on the left-hand side of figure 7 contains the butcher shop. The connecting block contains a cleaning facility, offices and building services. Figure 7 shows the building from direction north, starting with the incoming goods facility and figure 8 from the opposite side.

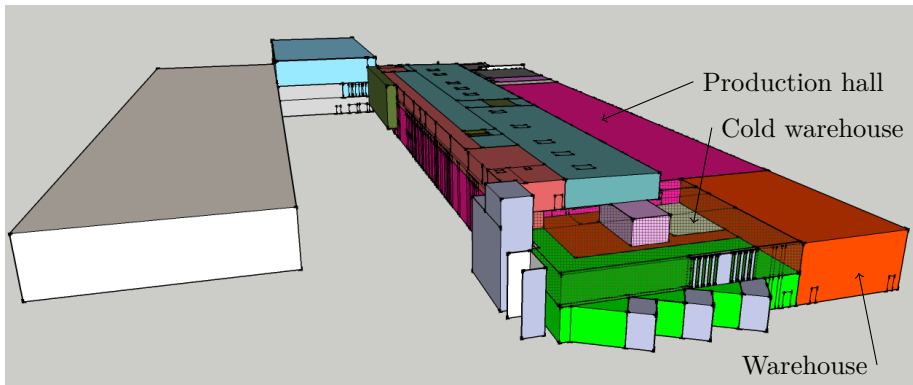


Figure 7: Building, view from north.

The EnergyPlus simulation divided the building into 24 thermal zones. In order to validate the proposed model, four distinct zones were chosen. These four zones have different characteristics, which are listed in table 2. The zone *cold warehouse* is the most basic zone of all four. It is not exposed to forced convection due to wind, nor solar radiation or infiltration. It is also the smallest of the chosen zones and is kept at a constant temperature of 4°C. This zone was chosen because it is the most basic zone and therefore it is possible to isolate effects and get helpful insights. The next zone is the zone *warehouse*. It is two-stories high and has an outer wall directed north and west without windows. The zone *warehouse* is kept at a constant temperature of 18°C. The zone *production hall* is also two-stories high and the largest zone of the building.

⁶More information on the Balanced Manufacturing project is available at www.bama.ift.tuwien.ac.at

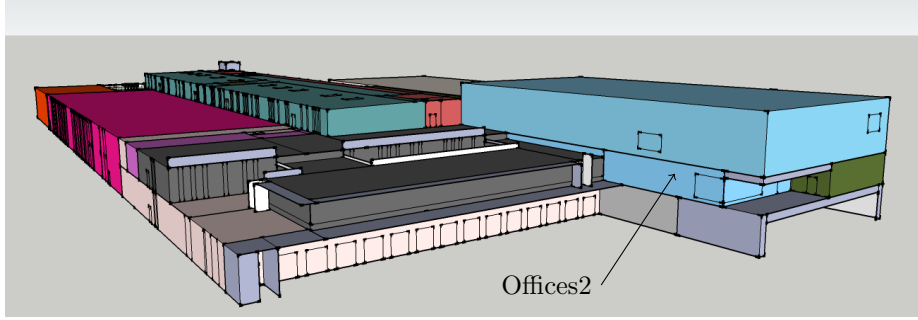


Figure 8: Building, view from south.

A quarter of the outer wall area are windows. The zone *production hall* is kept at a temperature range between 22 and 26°C. The last zone *offices2* is a single-story zone. The walls and windows of this zone are facing in the directions north, south and west. The window area is about 26% of the outer wall area and the temperature range is between 22 and 26°C.

Table 2: Overview of zone characteristics.

	Cold warehouse	Warehouse	Production hall	Offices2
Floor area	118 m ²	823 m ²	4916 m ²	785 m ²
Volume	554 m ³	5991 m ³	44158 m ³	3297 m ³
Outdoor wall area	0 m ²	412 m ²	1140 m ²	140 m ²
Window area as fraction of outdoor wall area	0 %	0 %	~25 %	~26 %
Infiltration rate	0 h ⁻¹	0.1 h ⁻¹	0.05 h ⁻¹	0.1 h ⁻¹
Setpoint temperature	4°C	18°C	22–26°C	22–26°C

5 Dymola model

With the increase in computing power runtime optimized thermal building simulations seem of little interest. However, their core strengths lie in the short computation time, easy expandability, user friendliness and straight forward approach [13]. The following model uses the RC analogy, in which thermal resistances and capacitances represent building characteristics. It is based on De Rosa et al. simplified model [18], which itself is based on the lumped capacitance approach [19] combined with electrical analogy [20]. Contrary to Nielsen's model, all properties of the model retain their physical properties⁷. Transient energy balance equations are set up for each wall, floor and roof as well as the internal air volume.

5.1 Energy balance for the internal air volume

A zone is modeled as single homogeneous isothermal air volume with a capacitance. The heat exchange with the inside of the walls (\dot{Q}_w), heating and cooling ($\dot{H}C$), internal gains (\dot{L}), infiltration (\dot{Q}_{inf}), conduction through windows and doors (\dot{Q}_{win}) as well as solar radiation (through the wall model) are taken into account. Figure 9 shows all modeled heat transfers for the internal air volume.

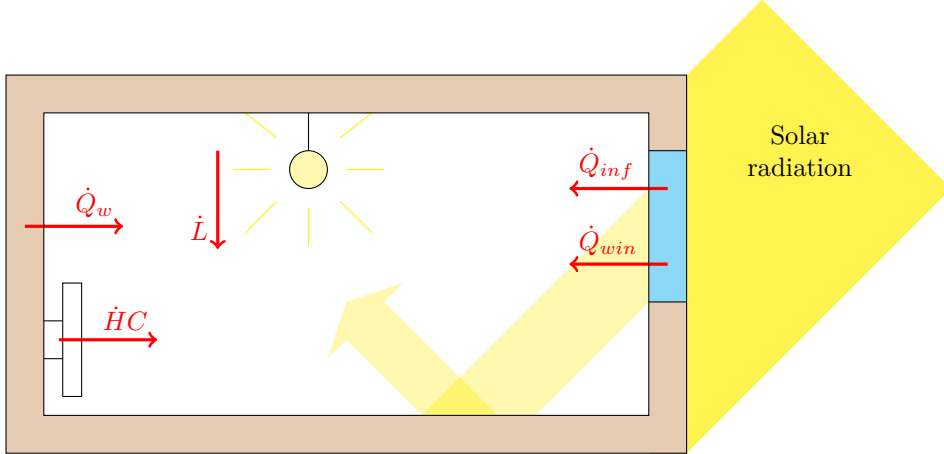


Figure 9: Schematic view of heat transfers in a zone.

The transient energy balance is solved at every time step. It is written as:

$$C_i \frac{dT_i}{dt} = \dot{H}C + \dot{L} + \dot{Q}_{inf} + \dot{Q}_w + \dot{Q}_{win} \quad (4)$$

- C_i is the heat capacity of air in the zone and is calculated via:

$$C_i = \rho_{air} V c_p. \quad (5)$$

Where ρ_{air} is the density of air, V the volume of the zone and c_p the specific heat capacity of air.

⁷In his model Nielsen uses a conductance (Kw) between heat capacity in constructions and internal surfaces which he states is *not well defined* and can be calculated by a not further defined equivalent thermal resistance.

- T_i is the uniform temperature of air in the zone.
- $\dot{H}C$ is the sensible heating or cooling power supplied to the zone in order to keep the zone air temperature within the set-point limits. It is considered to be purely conductive.
- \dot{L} is the free gain due to persons, lighting, equipment, etc.
- \dot{Q}_{inf} is the heat transfer through infiltration. It is calculated via:

$$\dot{Q}_{inf} = \rho_{air} V c_p n (T_{amb} - T_i) \quad (6)$$

where n is the infiltration rate.

- \dot{Q}_w is the heat transfer through walls and is calculated via:

$$\dot{Q}_w = - \sum_i \dot{q}_{i,i} - \sum_j \dot{q}_{ifloor,j} \quad (7)$$

Where $q_{i,i}$ and $q_{ifloor,j}$ are the heat flow rates on the wall's, respectively floor's, internal surface.

- \dot{Q}_{win} is the heat transfer through windows and doors. The thermal capacities of windows and doors are neglected due to their small influence. The heat transfer is purely conductive and is calculated via:

$$\dot{Q}_{win} = \sum_k U_k A_k (T_{amb} - T_i) \quad (8)$$

with the index k for the number of windows and doors.

5.2 Building envelope

A conventional wall consists of multiple physical wall layers. In the Dymola model each wall is divided into two halves, one facing inside the zone (internal layer), the other one facing outside (external layer). The internal layer exchanges heat with the zone air node, the external layer is exposed to external air convection and solar irradiation. Figure 10 shows the wall model in RC analogy. In the middle of the wall is the node capacitance point with the capacitance of all physical layers of a wall ($C_{w,i}$) and the wall temperature ($T_{w,i}$). The inside surface of the wall has the temperature $T_{i,i}$ and the outside surface the temperature $T_{e,i}$. Dividing the wall into two separate halves is one of the simplest wall discretizations and requires only one differential equation. However more complex discretizations with multiple capacitances are possible but lead to a higher amount of differential equations. It is to note that the node capacitance point does not necessarily has to be in the middle of the wall, it can also be placed, for example, after the insulation.

Figure 9 on page 17 shows how solar radiation is incorporated in the model. One part of the solar irradiation entering through the windows is absorbed by the floor(s), the reflected part is absorbed by the internal wall layer. The reflected irradiation is assumed to be uniformly distributed on all interior wall surfaces.

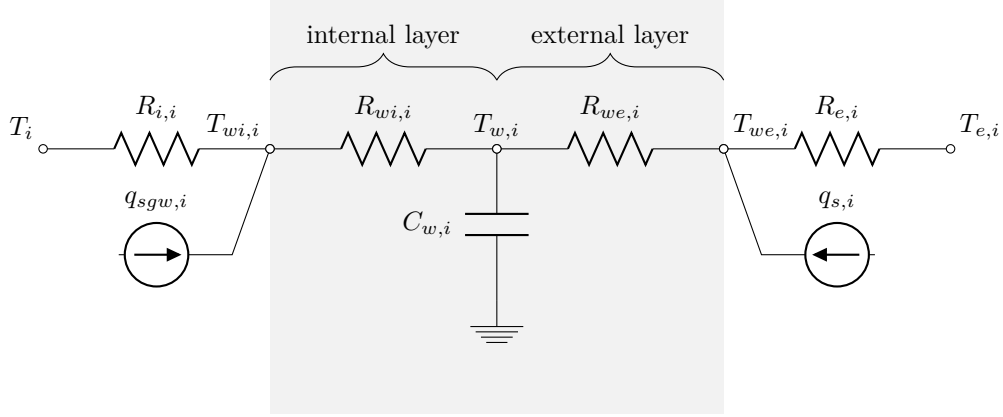


Figure 10: Wall model in electric analogy.

5.2.1 Energy balance for walls and ceilings

The transient energy balance is calculated at every time step and is written as:

$$C_{w,i} \frac{dT_{w,i}}{dt} = \dot{q}_{wi,i} + \dot{q}_{we,i} \quad (9)$$

- $C_{w,i}$ is the total capacitance of a wall and is calculated via:

$$C_{w,i} = \sum_k d_{k,i} \rho_{k,i} c_{k,i} A_i \quad (10)$$

Where $d_{k,i}$ is the thickness, $\rho_{k,i}$ the density, $c_{k,i}$ the specific heat and A_i the area of the wall.

- $T_{w,i}$ is the wall temperature in the middle of the wall.
- $\dot{q}_{wi,i}$ denotes the heat flux between the wall node and the internal wall surface.

$$\dot{q}_{wi,i} = \frac{T_{wi,i} - T_{w,i}}{R_{wi,i}} \quad (11)$$

- $T_{wi,i}$ is the interior surface temperature of the wall.
- $R_{wi,i}$ is the the conductive resistance of the internal wall layer.

$$R_{wi,i} = \sum_k \frac{s_k}{\lambda_k} \frac{1}{A_i} \quad (12)$$

Where the index k is the number of physical layers in the inner half of the wall, s_k the thickness of a layer and λ_k the thermal conductivity of the layer/material.

- $\dot{q}_{we,i}$ denotes the heat flux between the wall node and the external wall surface.

$$\dot{q}_{we,i} = \frac{T_{we,i} - T_{w,i}}{R_{we,i}} \quad (13)$$

- $T_{we,i}$ is the exterior surface temperature of the wall.
- $R_{we,i}$ is the the conductive resistance of the external wall layer. It is calculated the same way as the conductive resistance of the internal wall layer $R_{wi,i}$.
- The energy balances for the wall surfaces combine the heat flow rate on the internal or external surface with the solar contributions:

$$\dot{q}_{wi,i} = \dot{q}_{i,i} + \dot{q}_{sgw,i} \quad (14)$$

$$\dot{q}_{we,i} = \dot{q}_{e,i} + \dot{q}_{s,i} \quad (15)$$

Where

$$\dot{q}_{i,i} = \frac{T_i - T_{wi,i}}{R_{i,i}} \quad (16)$$

$$\dot{q}_{e,i} = \frac{T_{e,i} - T_{we,i}}{R_{e,i}} \quad (17)$$

- $R_{i,i}$ and $R_{e,i}$ are the inside and outside thermal resistances due to convection (contrary to $R_{wi,i}$ and $R_{we,i}$ which are purely conductive). They are calculated according to chapter 5.3 on page 21.

The calculation of $\dot{q}_{sgw,i}$ and $\dot{q}_{s,i}$ is conducted in chapter 5.7 on page 30.

5.2.2 Energy balance for floors

Floors are modeled similar to walls and ceilings with the difference that floors have no air convection and solar irradiation on the exterior surface⁸. Therefore the external heat flux is simply conductive.

The transient energy balance is calculated at every time step and is written as:

$$C_{wf,j} \frac{dT_{wf,j}}{dt} = \dot{q}_{wif,j} + \dot{q}_{wef,j} \quad (18)$$

- $C_{wf,j}$ is the total capacitance of a floor and is calculated via:

$$C_{wf,j} = \sum_k d_{k,j} \rho_{k,j} c_{k,j} A_j \quad (19)$$

Where $d_{k,j}$ is the thickness, $\rho_{k,j}$ the density, $c_{k,j}$ the specific heat of a floor layer and A_j the area of a floor.

- $T_{wf,j}$ is the temperature in the middle of the floor.
- $\dot{q}_{wif,j}$ denotes the heat flux between the floor node and the internal wall surface.

$$\dot{q}_{wif,j} = \frac{T_{wif,j} - T_{wf,j}}{R_{wif,j}} \quad (20)$$

- $T_{wif,j}$ is the surface temperature of the floor.

⁸For the floor model the exterior surface is the surface facing the ground.

- $R_{wif,j}$ is the the conductive resistance of the internal floor layer.

$$R_{wif,j} = \sum_k \frac{s_k}{\lambda_k} \frac{1}{A_j} \quad (21)$$

Where the index k is the number of physical layers in the inner half of the floor, s_k the thickness and λ_k the thermal conductivity of a floor layer.

- $\dot{q}_{wef,j}$ denotes the heat flux between the floor node and the ground.

$$\dot{q}_{wef,j} = \frac{T_{ground} - T_{wf,j}}{R_{wef,j}} \quad (22)$$

- T_{ground} is the surface temperature of the floor's outside. That is the temperature of the ground in direct contact with the floor.
- $R_{wef,j}$ is the the conductive resistance of the external floor layer. It is calculated the same way as the conductive resistance of the internal floor layer $R_{wif,j}$.
- The energy balance for the floor's surface combines the heat flow rate on the internal surface with the solar contributions onto the floor's surface:

$$\dot{q}_{wif,j} = \dot{q}_{ifloor,j} + \dot{q}_{sgf,j} \quad (23)$$

Where

$$\dot{q}_{ifloor,j} = \frac{T_i - T_{wif,j}}{R_{if,j}} \quad (24)$$

- $R_{if,j}$ is the inside thermal resistance due to convection. It is calculated according to chapter 5.3 on page 21.

$\dot{q}_{sgf,j}$ is calculated according to chapter 5.7 on page 30.

5.3 Convection

As there is no universally applicable wind convection coefficient model or correlation, convection is hard to model [21]. Therefore simulation programs often offer multiple convection coefficient models. De Rosa et al. used the well known MoWiTT model [23] which is especially suitable for low-rise buildings.

The resistances due to convection are calculated as follows:

$$R_{i,i} = \frac{1}{h_{i,i} A_{w,i}} \quad (25)$$

$$R_{e,i} = \frac{1}{h_{co,i} A_{w,i}} \quad (26)$$

$$R_{if,j} = \frac{1}{h_{if,j} A_{f,j}} \quad (27)$$

Where $R_{i,i}$, $R_{e,i}$ and $R_{if,j}$ are the resistances due to convection for the internal and external wall surface as well as the floor. A detailed explanation of the convection coefficients is given in the following section.

5.3.1 Convective heat transfer coefficients

The heat transfer coefficients are calculated according to the MoWiTT model. The MoWiTT model is based on a natural convection and a forced convection term.

“Because the transition region between natural and forced convection is poorly understood, there is no theoretical basis for combining natural and forced convection beyond the expectation that the film coefficient should vary continuously between the two regions.” [23, p.7f]

Therefore the the convection coefficient $h_{co,i}$ can simply be modeled as follows:

$$h_{co,i} = \sqrt{\underbrace{(3 + C_t |T_{e,i} - T_{we,i}|^{\frac{1}{3}})^2}_{\text{natural convection}} + \underbrace{(av_{ws}^b)^2}_{\text{forced convection}}} \quad (28)$$

A constant convection coefficient of $3\text{W}/(\text{m}^2\text{K})$ is added to the MoWiTT model in order to get a better resemblance of heating and cooling demand with the detailed EnergyPlus simulation, otherwise the interior convection coefficients would be too small. C_t , a and b are constants (see table 3). The constants a and b depend on wind-direction and are distinguished in windward and leeward. If the angle of incidence of wind on a wall is $< \pm 90^\circ$ the wall is considered windward, else it is considered leeward. v_{ws} is the wind-speed.

Table 3: Constants for calculation of convection coefficients [23, p.14].

Wind direction	C_t	a	b
Unit	$\text{W}/(\text{m}^2 \text{K}^{4/3})$	$\text{W}/(\text{m}^2 \text{K}) (\text{s}/\text{m})^b$	
Windward	0.84	3.26	0.89
Leeward	0.84	3.55	0.617

A plethora of different convection coefficient models is available. Two of them are presented briefly. For the sake of simplicity Palyvos [21] recommends a simple linear model for the convective heat transfer coefficients:

$$h_{co,i} = \begin{cases} 7.4 + 4.0 v_{ws} & \text{windward} \\ 4.2 + 3.5 v_{ws} & \text{leeward} \end{cases}$$

[22] for example uses a different approach based on the wind-speed:

$$h_{co,i} = \begin{cases} 4.0 v_{ws} + 5.6 & \text{for } v_{ws} \leq 5 \frac{\text{m}}{\text{s}} \\ 7.1 v_{ws}^{0.78} & \text{for } v_{ws} > 5 \frac{\text{m}}{\text{s}} \end{cases}$$

De Rosa et al. used a radiation term in addition to the convection coefficient to generate an external heat transfer coefficient $h_{tot,i}$ [18, appendix A]:

$$h_{tot,i} = h_{co,i} + h_{irr,i} \quad (29)$$

$$h_{irr,i} = \epsilon_{w,i} \sigma (T_{we,i}^2 + T_{e,i}^2) (T_{we} + T_e) \quad (30)$$

In this model the radiation term is completely neglected, due to its small impact on the overall heat transfer coefficient.

5.4 Windows and doors

Windows and doors are modeled identically. The thermal capacity of windows and doors is neglected and only a conductive heat flux is considered:

$$\dot{Q}_{win} = \sum_i \sum_k (T_{e,i} - T_i) U_{win,ik} A_{win,ik} \quad (31)$$

$T_{e,i}$ is the ambient (external) temperature of the i^{th} wall, index k the number of windows and doors of a wall, $U_{win,ik}$ the transmittance (u-value) of the window or door and $A_{win,ik}$ the area of the window or door. However one could consider a more complex model with an distinct RC network for the windows. Drawback is a considerable increase in computation time by a minor gain of accuracy.

5.5 Infiltration

Infiltration is calculated via:

$$\dot{Q}_{inf} = \rho_{air} V c_p n_{inf} (T_{amb} - T_i) \quad (32)$$

where n_{inf} is the infiltration rate⁹ and T_{amb} is the ambient temperature. Ventilation was not considered as the detailed EnergyPlus did not take ventilation into account. However, ventilation could easily be incorporated into the Dymola model.

5.6 Solar radiation on surfaces

This chapter contains a step-by-step guide for the calculation of the global solar radiation on a surface. First the apparent solar time is calculated in order to calculate the solar angles. Then the incidence angle and last the global solar radiation is calculated.

While this chapter contains the calculation of the global solar radiation in general, the next chapter (solar contributions) incorporates solar radiation into the Dymola model.

5.6.1 Reckoning of time

Apparent solar time (AST) is used in solar energy calculations to express the time of day rather than the local standard time (LST). AST is based on the motion of the sun while LST is based on a fictitious mean motion of the sun. The LST is corrected by the equation of time (ET) and longitude in order to

⁹The infiltration rate does not necessarily has to be constant over time. However as the detailed EnergyPlus simulation uses constant infiltration rates the proposed model also does.

calculate the *AST* [24]. The equation of time is caused by the obliquity of the ecliptic of earth and the eccentricity of the earth's orbit around the sun. It is obtained approximately via:

$$ET = 9.87 \sin(2B) - 7.53 \cos(B) - 1.5 \sin(B) \quad (33)$$

$$B = (N - 81) \frac{360}{364} \quad (34)$$

Where N is the day of the year (ranging from 1 to 365) and B a function linearly dependent on the day of the year. Figure 11 shows the trend of ET over a full year. If ET is greater than zero *AST* is ahead of *LST*.

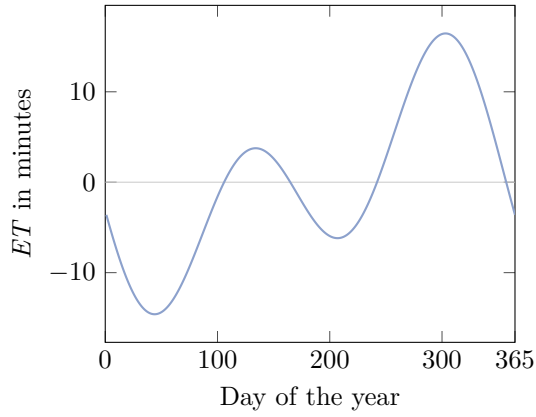


Figure 11: Equation of time.

The apparent solar time is calculated as follows:

$$AST = LST + \frac{ET}{60} \pm \underbrace{\frac{4(SL - LL)}{60}}_{\text{longitude correction}} - DS \quad (35)$$

Where the *LST* is corrected by the equation of time, by the longitude and optional the daylight saving time. As the sun takes four minutes to traverse 1° of longitude, hence the correction term is $4(SL - LL)$. SL is the standard longitude (15° for central european time) and LL the local latitude of the production facility in Tyrol (11.324°). West of the standard meridian the longitude correction term is subtracted, east of the standard meridian it is added. If using daylight saving time (DS) in the simulation the *AST* has to be corrected by 0 or 1h.

5.6.2 Solar angles

The position of the sun in the sky can be described (for an observer on earth) with two astronomical angles: the solar altitude (α) and solar azimuth (z). To put it in other words those two angles locate a point on the celestial sphere in the equatorial coordinate system (see figure 12). Beforehand the solar declination (δ) and hour angle (h) have to be calculated.

The solar declination represents the angle between the sun's rays and the equator. If the sun's rays are north of the equator the declination is positive. If

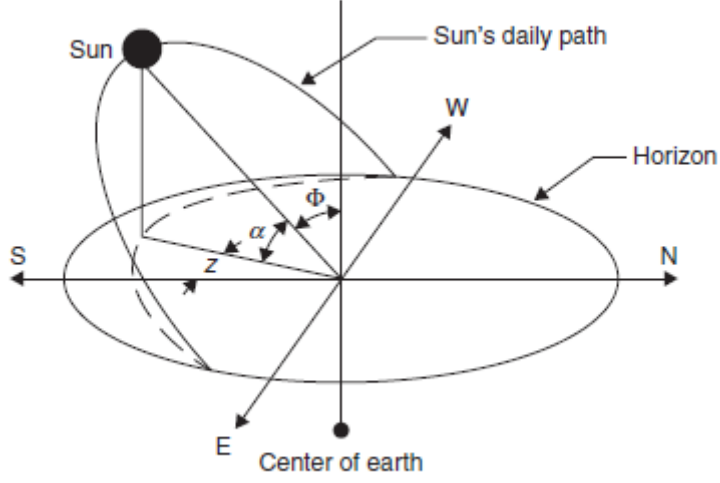


Figure 12: Daily path of the sun across the sky from sunrise to sunset [24, p.60].

they are south of the equator the declination is negative. The declination can be calculated approximately by equation (36). The declination over a year is shown in figure 13. The values of the declination stated below mark the limits of the astronomical seasons.

$$\delta = \begin{cases} +23.45^\circ & \text{at summer solstice} \\ 0^\circ & \text{at spring and fall equinox} \\ -23.45^\circ & \text{at winter solstice} \end{cases}$$

$$\delta = 23.45 \sin \left[\frac{360}{365} (284 + N) \right] \quad (36)$$

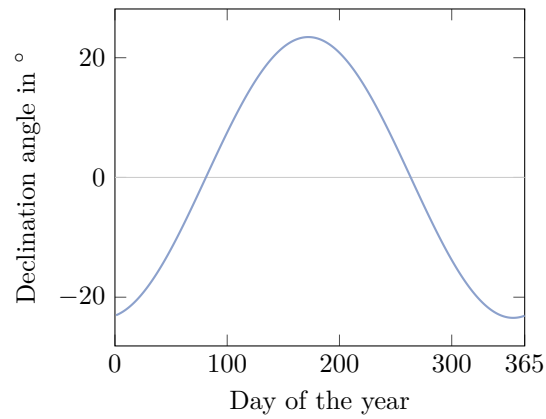


Figure 13: Declination of the sun.

The solar hour angle expresses the time-difference between AST and solar noon. The measurement of the hour angle is either in hours or in degrees. The earth rotates with 15° per hour, therefore one hour away from solar noon corresponds to a difference of 15° . Here the hour angle is calculated in degrees. The hour angle is per definition 0° at solar noon and is negative before solar noon and positive after solar noon.

$$h = (AST - 12)15 \quad (37)$$

Solar altitude angle

The solar altitude angle (α) is defined as angle between the sun's rays and a horizontal plane. Similar, the solar zenith angle (Φ) is defined as angle between the sun's rays and a vertical plane.

$$\Phi + \alpha = 90^\circ \quad (38)$$

The solar altitude and zenith angle are calculated via:

$$\sin(\alpha) = \cos(\Phi) = \sin(L) \sin(\delta) + \cos(L) \cos(\delta) \cos(h) \quad (39)$$

Where L is the local latitude of 47.253° for the analyzed production facility in Tyrol.

Solar azimuth angle

The solar azimuth angle (z) is defined as the angle between a line due south and the projection of the sun on a horizontal plane. There are 2 conventions for the solar azimuth angle. Here the solar azimuth angle is measured from south with positive angles towards westward. However the most commonly accepted convention is the observation from north with positive angles to the eastward direction. By adding 180° to the convention due south the solar azimuth angle can be converted to the convention due north. The solar azimuth angle can be calculated via:

$$\sin(z) = \frac{\cos(\delta) \sin(h)}{\cos(\alpha)} \quad (40)$$

However this equation is only correct for: $\cos(h) > \frac{\tan(\delta)}{\tan(L)}$. The following flowchart on page 27 gives a structured overview of the calculation of the solar azimuth angle. If $\cos(h) > \frac{\tan(\delta)}{\tan(L)}$ is false then the sun is behind the E-W line (see figure 12 on page 25). Therefore z has to be corrected by the formulas in the flowchart.

5.6.3 Incidence angle

The angle between the sun's rays and the normal of a surface is called solar incidence angle (θ). The general expression of the solar incidence angle is:

$$\begin{aligned} \cos(\theta) = & \sin(L) \sin(\delta) \cos(\beta) - \cos(L) \sin(\delta) \sin(\beta) \cos(Z_s) \\ & + \cos(L) \cos(\delta) \cos(h) \cos(\beta) \\ & + \sin(L) \cos(\delta) \cos(h) \sin(\beta) \cos(Z_s) \\ & + \cos(\delta) \sin(h) \sin(\beta) \sin(Z_s) \end{aligned} \quad (41)$$

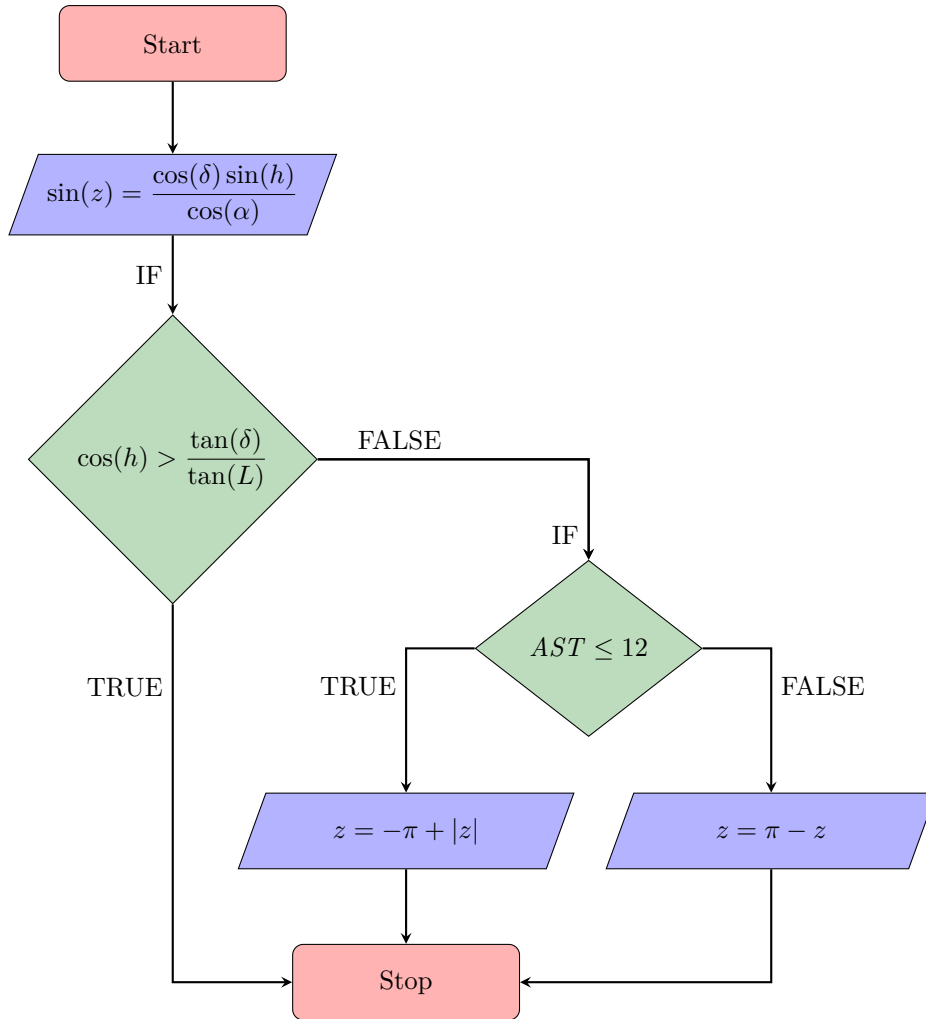


Figure 14: Calculation of the solar azimuth angle (z).

Where β is the tilt angle from the horizontal (e.g. 90° for a vertical wall) and Z_s the angle between the normal of a surface to true south (surface azimuth angle).

$$Z_s = \begin{cases} +180^\circ & \text{north} \\ +270^\circ & \text{east} \\ 0^\circ & \text{south} \\ +90^\circ & \text{west} \end{cases}$$

The Z_s values for each cardinal direction are stated above. The direction westward from south is designated positive while eastward is designated negative. For specific cases equation (41) can be reduced to simpler forms. For vertical surfaces ($\beta = 90^\circ$) it is reduced to:

$$\begin{aligned} \cos(\theta) = & -\cos(L) \sin(\delta) \cos(Z_s) + \sin(L) \cos(\delta) \cos(h) \cos(Z_s) \\ & + \cos(\delta) \sin(h) \sin(Z_s) \end{aligned} \quad (42)$$

For horizontal surfaces ($\beta = 0^\circ$) $\theta = \Phi$ applies.

5.6.4 Solar radiation on surfaces

In most cases radiation data is only available for the horizontal plane, therefore it has to be converted for sloped surfaces. Here the global solar radiation I_i is the sum of the beam component, diffuse component and ground reflected component:

$$I_i = \underbrace{I_{b,n} \cos(\theta)}_{\text{beam}} + \underbrace{I_{d,n}}_{\text{diffuse}} + \underbrace{(I_{b,n} \sin(\alpha) + I_{d,h}) \xi_{r,w}}_{\text{ground reflected}} \quad (43)$$

Where $I_{b,n}$ is the normal direct solar radiation. $I_{d,n}$ is the diffuse solar radiation which can be modeled by a plethora of isotropic, pseudo-isotropic and anisotropic models. An overview of these models is found in [25]. $I_{d,h}$ is the horizontal diffuse solar radiation. Both, $I_{b,n}$ and $I_{d,h}$ originate from measured data while $I_{d,n}$ has to be approximated by the above stated models. $\xi_{r,w}$ is the tilt solar redirected radiation factor and is calculated via:

$$\xi_{r,w} = \rho \frac{1 - \cos(\beta_i)}{2} \quad (44)$$

Where ρ is the ground reflectivity or ground surface albedo. Here a constant ground reflectivity of 0.2 is assumed [26, 27]. β_i is the surface tilt angle (e.g. 90° for a vertical wall).

For the diffuse solar radiation the Perez model was used. The Perez model is an anisotropic model and very popular due to its accurate results and easy calculation. The Perez model divides the diffuse solar radiation in 3 terms: the region over the horizon, the circumsolar region and the rest of the isotropic sky dome.

$$I_{d,n} = \underbrace{I_{d,h} F_2 \sin(\beta_i)}_{\text{horizon}} + \underbrace{I_{d,h} (1 - F_1) \frac{1 + \cos(\beta_i)}{2}}_{\text{dome}} + \underbrace{I_{d,h} F_1 \frac{a}{b}}_{\text{circumsolar}} \quad (45)$$

Where F_1 and F_2 are functions for the circumsolar brightness coefficient respectively horizon brightness coefficient. The coefficients a and b are incidence angles which are limited by a maximum function in order to give reasonable

results for zenith angles higher than 85° . Reason is that the horizontal diffuse solar radiation is divided by the cosine of the zenith angle (see equation (45)) for the circumsolar term of the diffuse solar radiation. If the position of the sun is very low, between 85 and 90° , the cosine of this angle approaches zero and therefore results in way too high values for the diffuse solar radiation [28].

$$a = \max(0, \cos(\theta)) \quad (46)$$

$$b = \max(0.087, \cos(\Phi)) \quad (47)$$

Note that instead of 0.087 the term $\cos(85^\circ)$ is often used in literature.

As F_1 and F_2 are functions of the relative optical air mass (m), the sky's clearness (ϵ) and the sky's brightness (Δ) the calculation of the necessary values is presented below.

The relative optical air mass is the direct optical path length through the earth's atmosphere defined as the ratio of path length to the path length at the zenith. Here the approximation according to [29] is used:

$$m = \frac{1}{\cos(\Phi) + 0.50572(96.07995 - \Phi)^{-1.6364}} \quad (48)$$

According to [30] the sky's brightness and clearness are calculated as:

$$\Delta = I_{d,h} \frac{m}{I_0} \quad (49)$$

Where I_0 is the extraterrestrial irradiance.

The sky's clearness is calculated via:

$$\epsilon = \frac{\frac{I_{d,h} + I_{b,n}}{I_{d,h}} + \kappa \Phi^3}{1 + \kappa \Phi^3} \quad (50)$$

Where $\kappa = 1.041$. Note that this equation uses Φ in radians (whereas in the other equations it is used in degrees). The values for the sky's clearness are afterwards assigned to the clearness ranges (ϵ_{bin}) in table 4. The clearness range goes from overcast to clear sky.

Table 4: Discrete sky clearness categories [30, p.273].

ϵ_{bin}	Category	lower bound	upper bound
1	Overcast	1	1.065
2	.	1.065	1.230
3	.	1.230	1.500
4	.	1.500	1.950
5	.	1.950	2.800
6	.	2.800	4.500
7	.	4.500	6.200
8	Clear	6.200	

F_1 and F_2 are calculated as follows:

$$F_1 = F_{11} + F_{12}\Delta + F_{13}\Phi \quad (51)$$

$$F_2 = F_{21} + F_{22}\Delta + F_{23}\Phi \quad (52)$$

Where F_{11} - F_{23} are empirically obtained constants depending on the range of the sky's clearness (ϵ_{bin}) and Φ in radians. The constants F_{11} - F_{23} are shown in table 5. Note, a higher precision table can be found in [16].

Table 5: Perez model coefficients [30, p.282].

ϵ_{bin}	F_{11}	F_{12}	F_{13}	F_{21}	F_{22}	F_{23}
1	-0.008	0.588	-0.062	-0.060	0.072	-0.022
2	0.130	0.683	-0.151	-0.019	0.066	-0.029
3	0.330	0.487	-0.221	0.055	-0.064	-0.026
4	0.568	0.187	-0.295	0.109	-0.152	-0.014
5	0.873	-0.392	-0.362	0.226	-0.462	0.001
6	1.132	-1.237	-0.412	0.288	-0.823	0.056
7	1.060	-1.600	-0.359	0.264	-1.127	0.131
8	0.678	-0.327	-0.250	0.156	-1.377	0.251

The solar radiation on a surface can now be calculated via equation (43) on page 28.

5.7 Solar contributions

Solar contributions are modeled for opaque walls and through windows.

5.7.1 Solar radiation on opaque walls

The heat contribution of solar radiation on the exterior side of a wall is calculated via:

$$\dot{q}_{s,i} = \alpha_{w,i} A_{w,i} I_i \quad (53)$$

Where $\dot{q}_{s,i}$ is the heat flux of solar radiation on an exterior wall, $\alpha_{w,i}$ is the outer solar absorbance coefficient, $A_{w,i}$ the area of the wall and I_i the global solar radiation.

5.7.2 Solar radiation through windows

The total solar radiation transmitted through the windows \dot{q}_{sg} is calculated via:

$$\dot{q}_{sg} = \sum_i f_i \tau_{win,i} A_{win,i} I_i \quad (54)$$

Where f_i is the factor of shading which ranges from 0 (complete shading - no solar radiation enters the room) to 1 (no shading). Here shading was neglected (therefore set to 1) in order to keep the model as simple as possible. Note that the windows are shaded by fixed fins and the shading factor can be calculated by the sun's position (see chapter 5.6.2) and the geometry of the fins. $\tau_{win,i}$ is the glass transmission coefficient and $A_{win,i}$ the total window area of a wall.

The model assumes that most of the entering solar radiation is absorbed by the floor with the floor's absorbance $\alpha_{f,j}$. The rest of the solar radiation is reflected onto the interior walls and ceilings (see figure 9 on page 17). The

distribution of the reflections is assumed to be equally distributed on all interior surfaces (except the floor).

$$\dot{q}_{sgf,j} = \alpha_{f,j} \dot{q}_{sg} \quad (55)$$

$$\dot{q}_{sgw,i} = \frac{A_{w,i}}{\sum_i A_{w,i}} (1 - \bar{\alpha}_f) \dot{q}_{sg} \quad (56)$$

Where $\dot{q}_{sgf,j}$ and $\dot{q}_{sgw,i}$ are the heat fluxes due to solar radiation on the floor, respectively on the walls. $\alpha_{f,j}$ is the inner solar absorptance of a floor and $\bar{\alpha}_f$ is the average inner solar absorptance per square-meter of a floor if multiple floors are present (e.g. the zones floor consists of two or more different floors in terms of construction).

5.8 Initialization of the model

The proposed model seems to be complete at this point. However the differential equations (4), (9) and (18) need initial values for their derived temperatures T_i , $T_{w,i}$ and $T_{wf,j}$. As the simulation spans a full year, starting on the 1st of January, the zone air temperature is supposed to be at the lower set-point temperature. The case gets more complex for the wall and floor node temperatures. A first approximation would set the initial values for the wall and floor nodes to the arithmetic mean of the exterior and indoor temperature:

$$T_{w,i} = \frac{T_{e,i} + T_i}{2} \quad (57)$$

$$T_{wf,i} = \frac{T_{ground} + T_i}{2} \quad (58)$$

We see that the wall node temperatures need the initial zone air temperature as input in the equation. The problem with this simple solution is that in most cases the conduction resistances of the wall $R_{wi,i}$ and $R_{we,i}$ as well as the conduction resistances of the floor $R_{wif,j}$ and $R_{wef,j}$ are not equal and will result in an incorrect wall temperature, which distorts the results of the simulation in the first few days or even weeks (see figure 15).

Therefore the wall and floor node temperatures have to be weighted by the respective conduction resistances:

$$T_{w,i} = \frac{\frac{T_{e,i}}{R_{we,i}} + \frac{T_i}{R_{wi,i}}}{\frac{1}{R_{we,i}} + \frac{1}{R_{wi,i}}} \quad (59)$$

$$T_{wf,i} = \frac{\frac{T_{ground}}{R_{wef,j}} + \frac{T_i}{R_{wif,j}}}{\frac{1}{R_{wef,j}} + \frac{1}{R_{wif,j}}} \quad (60)$$

A comparison for the different initial wall temperature methods is shown in figure 16 on page 33. Here the trend of the wall temperature for a wall of the zone *production hall* is shown for the simple and more complex method. The wall is exposed to an indoor temperature of 22°C and a constant exterior temperature of 4°. With the simple initial formula the wall temperature needs about 300 hours to tune in, while the more complex initial formula leads to a smaller difference of starting temperature and converged temperature. Furthermore

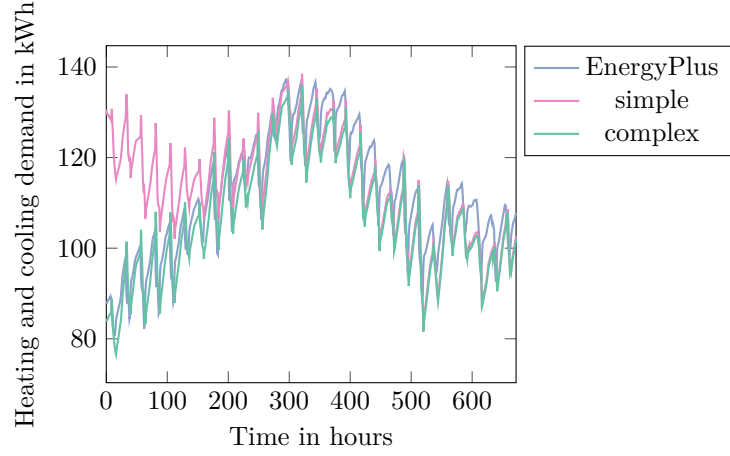


Figure 15: Heating and cooling demand for different initial values.

the influence of initial values is especially crucial for short term simulations, because it only influences the first few days or weeks. Looking at figure 15 we see that there is a discrepancy between the results of the starting period and the reference simulation which diminishes over time. However there are different solutions to remedy the initial value problem:

- Cutting the first few hours or weeks (dummy period). This means that a full period is simulated, but only the period time minus the dummy period is considered. However, in most cases the simulation results for the full year or period are necessary.
- Mirroring the climate data for a dummy period. The climate data is mirrored and the dummy period is put before the actual simulation increasing the simulated time by the dummy period. The advantage of this method is that no additional climate data is necessary and the temperature trend is continuous [31].

Figure 17 shows the heating demand for the zone *production hall*, with and without a mirrored dummy period, for the first four days of the year. We see that the used dummy period of seven weeks (before the actual start of the simulation) does not lead to better results than the complex initial value method in this particular case.

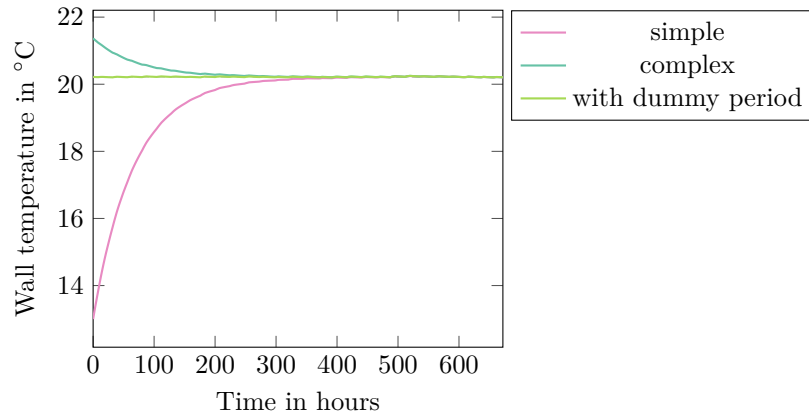


Figure 16: Wall temperature for different initial values.

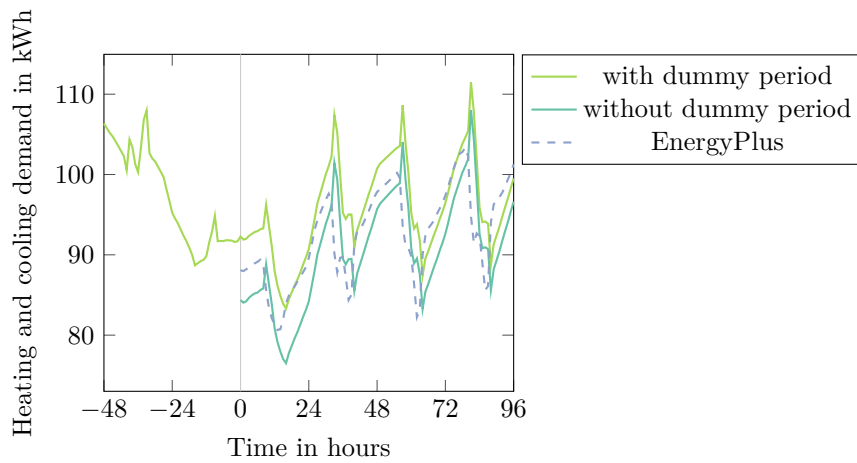


Figure 17: Heating and cooling demand with and without dummy period.

6 Comparison of the Dymola model to the reference simulation

The results of the presented model are now compared to the detailed EnergyPlus simulation. The detailed EnergyPlus simulation uses a time step of a quarter of an hour, the presented model of one hour. Therefore the results of the EnergyPlus simulation are averaged over an hour in order to compare the results. However, the time step of the presented model can be adjusted freely, but the environment data is only available in hourly time steps and the data has to be interpolated for shorter time steps than one hour¹⁰. In this chapter the heating and cooling demand of four building zones are compared to the detailed EnergyPlus simulation over a full year, as well as the zone air temperatures.

6.1 Detailed convection model

The presented Dymola model is called the detailed convection model because a simple convection model was also analyzed. The results of the model are shown in figure 18 and 19. Table 6 lists the deviation of the summed yearly heating, cooling and combined energy demand as well as the root-mean-square error (RMSE) and the mean bias error (MBE). The RMSE is a measure of average deviation from a *true value*. Here the true value are the results from the detailed EnergyPlus simulation (in other cases from the detailed convection model). The RMSE is calculated as follows:

$$RMSE = \sqrt{\frac{\sum_{k=1}^n (x_k - x_{true})^2}{n}} \quad (61)$$

The MBE is a measure of overall bias error and calculated as follows:

$$MBE = \frac{1}{n} \sum_{k=1}^n x_k - x_{true} \quad (62)$$

Where n is the number of samples, x_k the simulated value and x_{true} the true value. Both, the RMSE and the MBE, are absolute values in Wh/m². Therefore they can easily be compared to the presented diagrams. However the RMSE and MBE are not normalized, therefore these values cannot be compared directly between the different zones but they can be compared for different models.

Looking at the plotted results of the model (see figure 18), one can see that the proposed model has little deviation to the course of the detailed EnergyPlus simulation. Especially the heating demand shows very little overall deviation to the reference simulation (the maximum deviation of heating demand is 4.36 %). Taking a closer look at the cooling demand we notice that the peaks of the proposed model are higher than those of the reference simulation. The overall cooling demand is significantly higher. In the zone *production hall* it is 109.5 % higher. Fixed fins in front of the windows reduces solar gains. The shading through these fins is not taken into account in the model. However the cooling

¹⁰Note that environment data is normally available in one hour time steps and simulation suites like EnergyPlus also have to interpolate the environment data for shorter simulation time steps.

demand is only a very small fraction of the total energy demand (except for the zone cold warehouse).

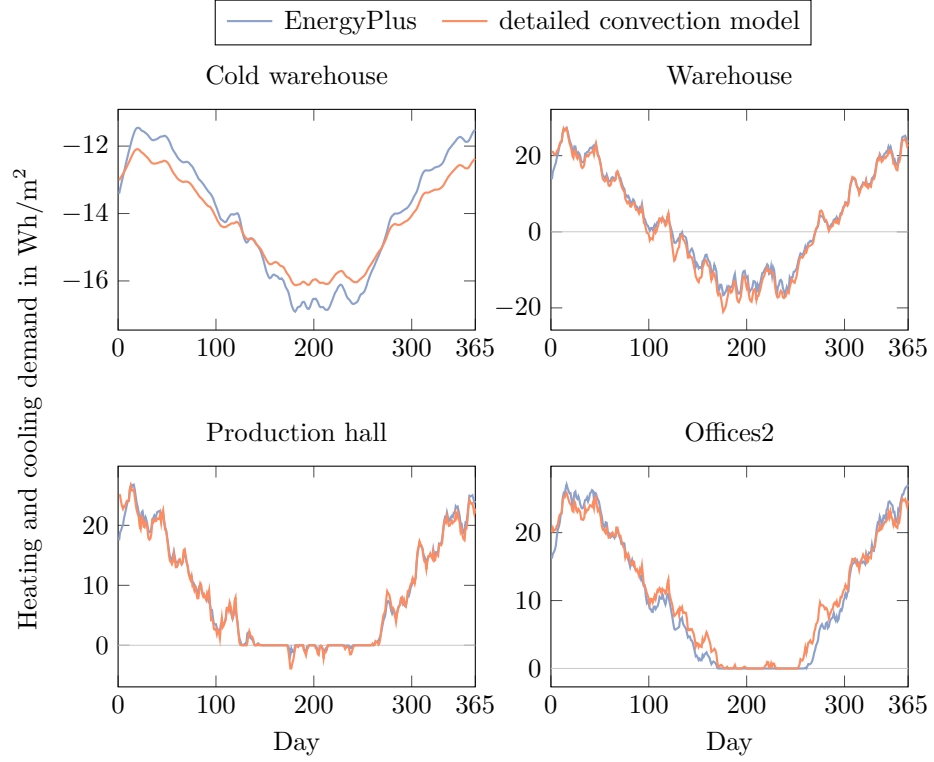


Figure 18: Daily average of heating and cooling demand for detailed convection model.

The zone *cold warehouse* seems to have a smaller dynamic range than the reference simulation. This zone is not exposed to the outdoor environment, only to other zones. All of these zones have a constant temperature, except one (which is not heated or cooled either). There is no (modeled) infiltration in this zone either. This leaves the conclusion that the heat flux through the unconditioned zone is modeled too small due to an incorrect convection coefficient, as there is no solar radiation distorting the heat flux through the wall. Figure 22 on page 42 shows the zone *cold warehouse* modeled with different constant convection coefficients. One notices that the higher the convection coefficients get the closer the trends of the cooling demand get in terms of dynamic range. With a constant convection coefficient of $100 \frac{W}{m^2 K}$ the trend of the simulation has the same dynamic as the reference simulation. Note that this is only valid for the zone *cold warehouse*, because the walls are only subjected to a constant outside temperature and therefore the higher convection coefficients only lead to a higher bias. In the other zones overly high convection coefficients lead to a higher heating and cooling demand, making the trend of the heating and cooling demand steeper than it would be in reality.

The air temperatures of the zones have a good resemblance with the reference

simulation. Note that the zones *cold warehouse* and *warehouse* have constant temperatures, therefore they are not plotted. The zones *production hall* and *offices2* have a temperature range of 22 to 26°C. Only the zone *production hall* reaches the temperature limit (upper set-point temperature). It shows little deviation to the reference simulation, while the zone *offices2* has a bias of about -1°C. However despite the bias it shows a similar trend to the reference simulation.

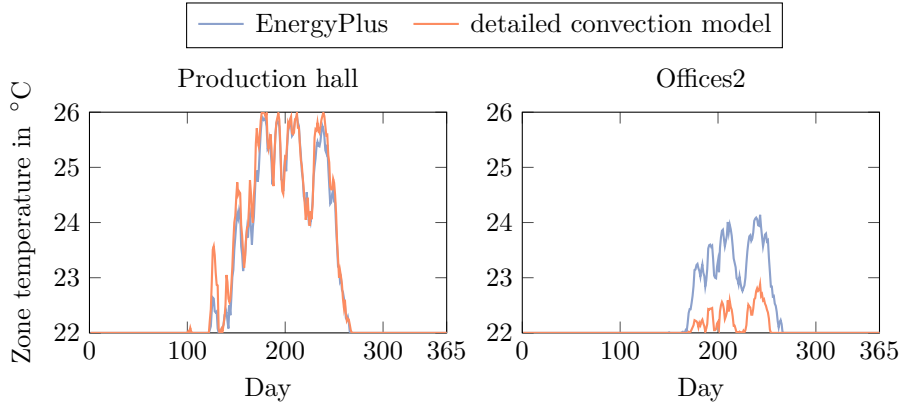


Figure 19: Daily average of zone temperatures for detailed convection model.

Overall the presented model shows a very good resemblance to the substantially more detailed EnergyPlus model. Especially the heating demand is calculated very accurately. Taking the effects of the untended shading through fixed fins into account the already minor negative MBE would probably reach zero and the deviation to the reference simulation would be furthermore reduced. The presented model proved to be a useful tool in order to evaluate the heating and cooling demand of a zone.

Table 6: Deviation of detailed convection model to the reference simulation.

Difference to EnergyPlus model	Cold warehouse	Ware-house	Production hall	Offices2
Heating demand		-3.62%	-1.36%	+4.36%
Cooling demand	+0.99%	+19.89%	+109.50%	
Combined heating and cooling demand	+0.99%	+4.28%	-0.68%	+4.36%
RMSE	0.54	1.72	1.39	1.65
MBE	-0.14	-1.06	-0.18	0.47

The presented Dymola model showed low required computation times. However, the required computation time increases drastically with the number of walls. A detailed overview and discussion on the required computation time is given in chapter 7.8.

7 Model simplifications

The presented model is already pretty simple but it can be reduced even more. If further simplifications are feasible and to what degree is shown in this chapter. The convection model and the floor model are simplified. Furthermore the influence of solar radiation and wall's thermal capacitance are shown, as well as a lumped wall model and a minimal model. At the end of the chapter the required computation times are compared to each other.

7.1 Simple convection model

In the simple convection model the natural convection term of the convection coefficient $h_{co,i}$ is replaced by a constant convection coefficient of $3 \text{ W}/(\text{m}^2\text{K})$:

$$h_{co,i} = \sqrt{3^2 + (av_{ws}^b)^2} \quad (63)$$

Several constant convection coefficients were tested and compared to the EnergyPlus simulation. A constant convection coefficient of $3 \text{ W}/(\text{m}^2\text{K})$ resulted in the most accurate results of all tested coefficients and is a realistic assumption. This simplification is motivated by a huge reduction in computation time (see chapter 7.8).

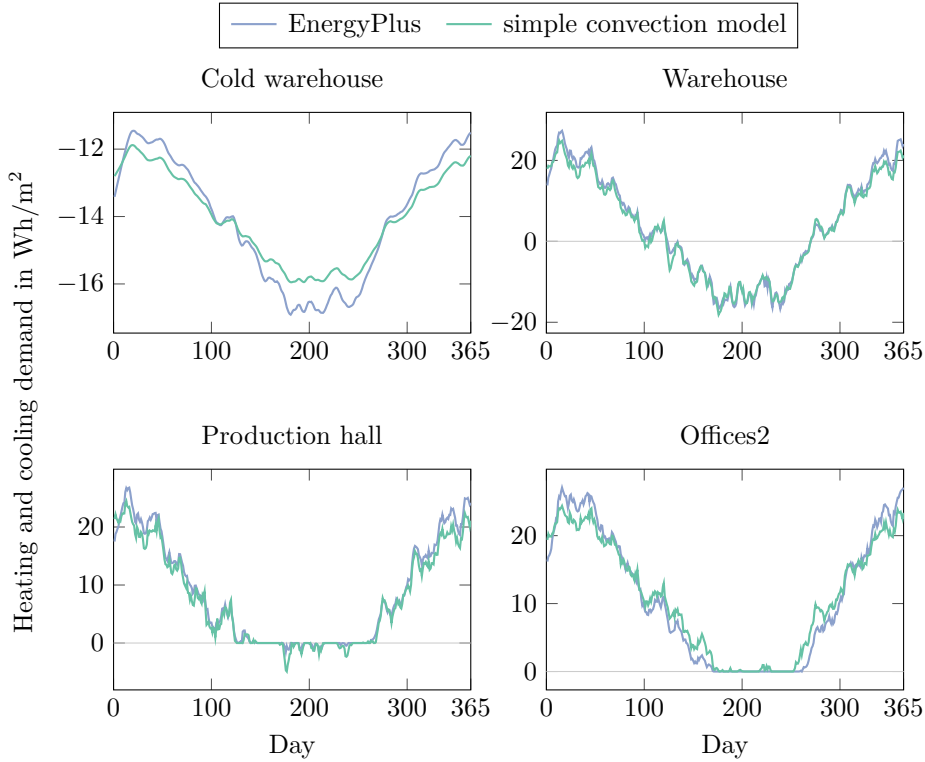


Figure 20: Daily average of heating and cooling demand for simple convection model.

Figure 20 shows the heating and cooling demand for the simple convection model and the EnergyPlus simulation. One notices the close resemblance to the presented Dymola model (see figure 18). As there is little difference for the heating and cooling demand of the detailed and simple convection model, the values in table 7 help to analyze the results. First of all the simplified convection model shows the highest differences to the EnergyPlus simulation in every aspect compared to the detailed convection model. However some values are closer to the EnergyPlus simulation than the detailed convection model, namely the deviation of cooling demand in the zones *cold warehouse* and *warehouse* as well as the heating demand of the zone *offices2*. The fact that the simpler convection model is sometimes more accurate than the detailed convection model is caused by the convection model. The high amount of uncertainty makes the convection model error-prone. Also the RMSE and MBE are lower for the zones *cold warehouse* and *warehouse* (closer resemblance of the trends) and higher in the zone *production hall* (lower resemblance). In the zone *offices2* the MBE of the simple model is lower and the RMSE is higher than in the detailed model. This means that the curve is closer to the EnergyPlus simulation but with higher deviation to it. Note that the cooling demand of the zone *production hall* is about 200 % larger than the reference simulation while the detailed convection model is about 110 % larger. However the simplified convection model is still a very good approximation to the reference simulation. Here the constant (natural) convection coefficient of $3 \text{ W}/(\text{m}^2\text{K})$ works very well. A different building with different building characteristics and environment may need a different value for the constant convection term. Approximating or validating the simplified convection model with a detailed convection model is highly advised and little additional effort.

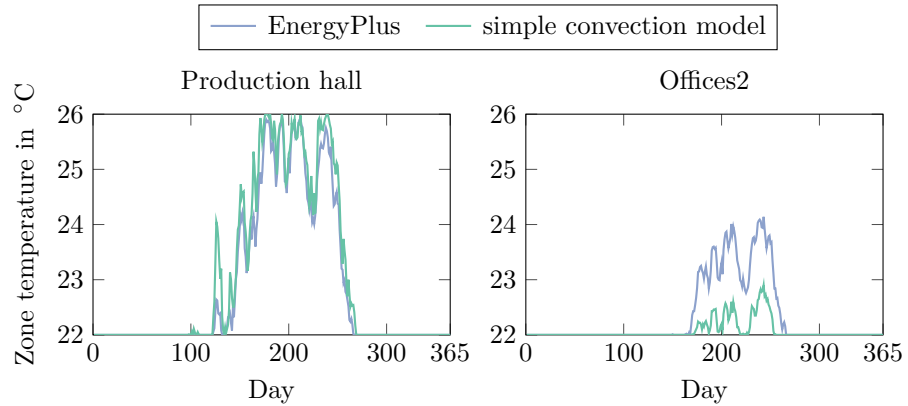


Figure 21: Daily average of zone temperatures for simple convection model.

The temperature trend is very similar to the detailed convection model, showing only minor deviations to it (compare to figure 19).

Table 7: Deviation of simple convection model to the reference simulation.

Difference to EnergyPlus model	Cold warehouse	Ware- house	Production hall	Offices2
Heating demand		-8.91%	-9.92%	+1.35%
Cooling demand	-0.26%	+2.49%	+199.86%	
Combined heating and cooling demand	-0.26%	-5.08%	-8.64%	+1.35%
RMSE	0.52	1.52	1.98	1.97
MBE	0.04	-0.79	-0.97	0.15

7.2 Constant convection coefficients

The simplified convection model is furthermore simplified by replacing all convection coefficients by a constant value. The convection coefficients of 5, 10 and $100 \text{ W}/(\text{m}^2\text{K})$ are used. Therefore the effect of forced convection due to wind is not modeled. Also the value of $100 \text{ W}/(\text{m}^2\text{K})$ is only used for testing purpose rather than realistic assumption (the highest convection coefficients in the simulations lied in the area of $30\text{--}37 \text{ W}/(\text{m}^2\text{K})$ for short periods of time).

Figure 22 for the heating and cooling demand for different constant convection coefficients shows that this simplification is only acceptable for zones which are not subject to forced convection (wind), here this is the zone *cold warehouse*. In the zone *production hall* the cooling demand for a convection coefficient of $5 \text{ W}/(\text{m}^2\text{K})$ is 2377% higher than the reference EnergyPlus simulation because this zone has a very low cooling demand. The influence of convection coefficients is in detail discussed in section 6.1. We see that the results generally differ more the greater the convection coefficient gets. Also the RMSE and MBE values in table 8 show the large discrepancy between the model's results and the reference simulation.

Comparing the results of the model with the constant convection coefficient of $100 \frac{\text{W}}{\text{m}^2\text{K}}$ to the minimal model (see chapter 7.7) - a model that only takes conduction into account - we see a very close resemblance. The results are not surprising. The higher the convection coefficient, the lower the inside and outside convection resistances get. An infinite convection coefficient leads to a convective resistance of zero, therefore no convection at all. Note that not only the heating and cooling demands of the model with the highest convection coefficient but also the zone temperatures are very similar to those of the minimal model.

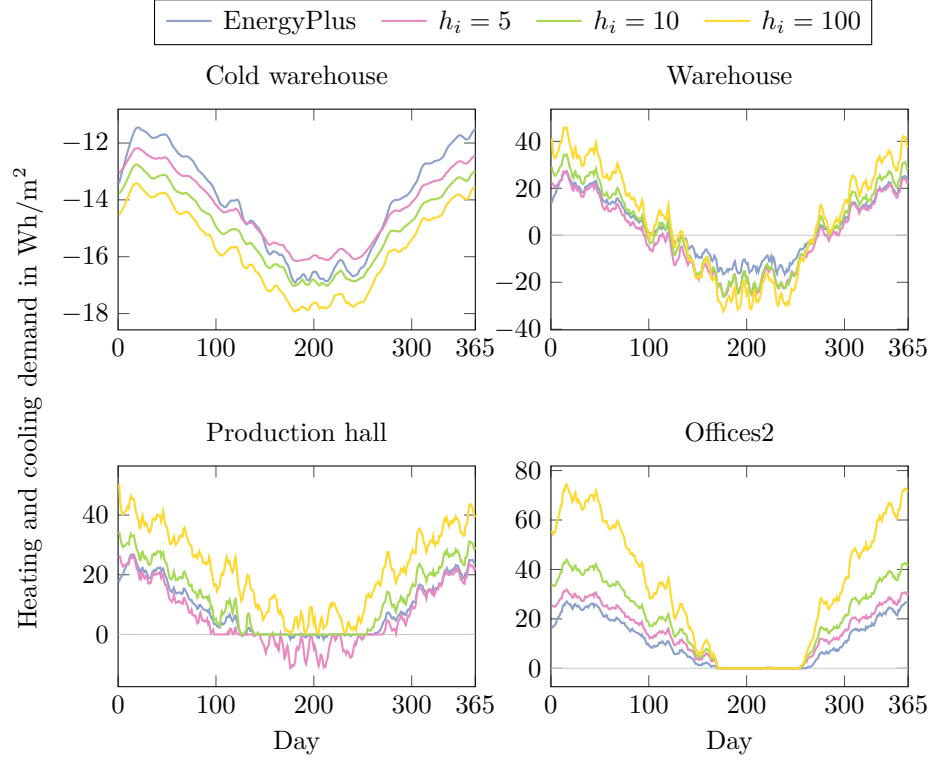


Figure 22: Daily average of heating and cooling demand for various convection coefficients.

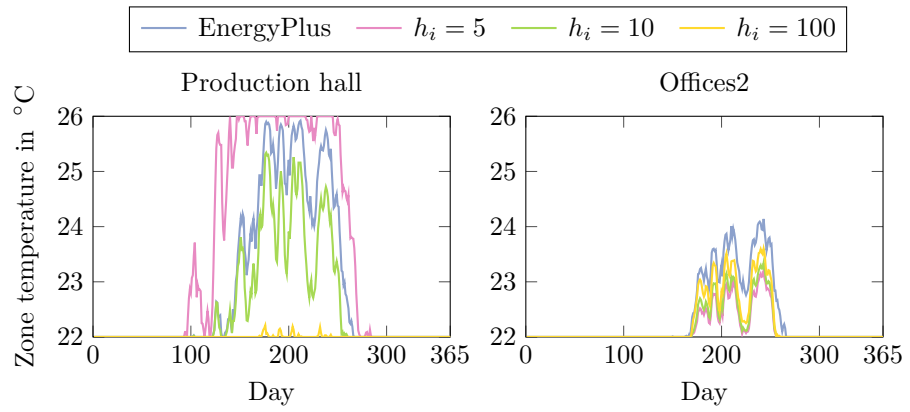


Figure 23: Daily average of zone temperatures for various convection coefficients.

Table 8: Deviation of various convection coefficients to the reference simulation.

Difference to EnergyPlus model	convection coefficient	Cold warehouse	Ware- house	Production hall	Offices2
Heating demand	$h_i = 5$		-11.55%	-15.36%	+29.67%
	$h_i = 10$		+23.61%	+37.21%	+78.86%
	$h_i = 100$		+75.41%	+150.86%	+200.84%
Cooling demand	$h_i = 5$	+1.35%	+74.82%	+2377.34%	
	$h_i = 10$	+6.41%	+56.44%	-100.00%	
	$h_i = 100$	+11.58%	+88.75%	-100.00%	
Combined heating and cooling demand	$h_i = 5$	+1.35%	+17.46%	-0.81%	+29.67%
	$h_i = 10$	+6.41%	+34.64%	+36.37%	+78.86%
	$h_i = 100$	+11.58%	+79.89%	+149.34%	+200.84%
RMSE	$h_i = 5$	0.57	4.89	3.82	3.76
	$h_i = 10$	1.01	4.80	4.29	10.29
	$h_i = 100$	1.67	10.53	14.38	27.14
MBE	$h_i = 5$	-0.19	-3.82	-2.60	3.19
	$h_i = 10$	-0.90	-0.38	3.29	8.48
	$h_i = 100$	-1.63	2.36	13.16	21.59

7.3 Simple floor model

Instead of the complex floor model (see chapter 5.2.2) with one capacitance, two internal conduction resistances and one internal convective resistance and solar gain, the floor is modeled simply with one conductive resistance. Therefore the heat transfer into the ground is modeled as follows:

$$\dot{q}_{i\text{floor},j} = \frac{1}{\sum_k R_k} A_j (T_i - T_{\text{ground}}) \quad (64)$$

Where j is the index variable for the floor, k the number of layers of a floor and R_k the respective conductive resistances. This reduces the model by one differential equation and three equations. Figure 24 shows a very good resemblance between the proposed Dymola model (detailed convection model) and the simplified floor model. All deviations except the cooling demand of the zone *production hall* are minor. The cooling demand of the zone *production hall* is overestimated by about 82 % compared to the Dymola model.

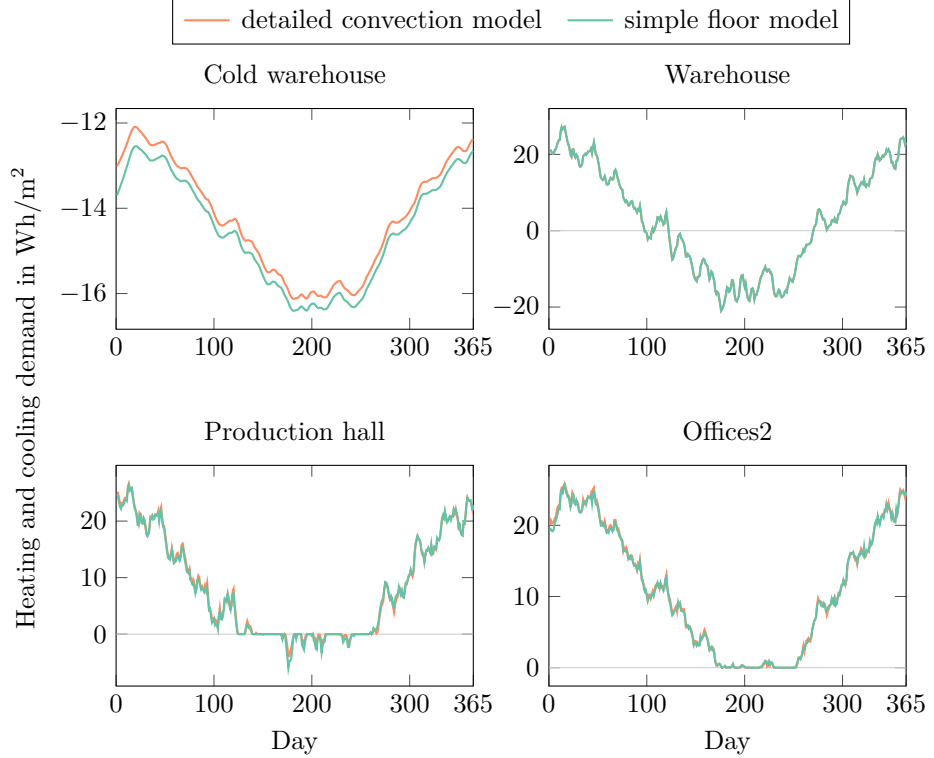


Figure 24: Daily average of heating and cooling demand for simple floor model.

The temperature trends of the simplified floor model (see figure 25) also show a good resemblance, but result in slightly higher zone temperatures. The higher temperatures are caused by the missing of the thermal capacity of the floor.

The MBEs of the simple floor model (see table 9) are negative for most zones, caused by a higher cooling demand. The RMSEs are generally very low. Compared to the detailed convection model in table 6 the simplified floor model shows

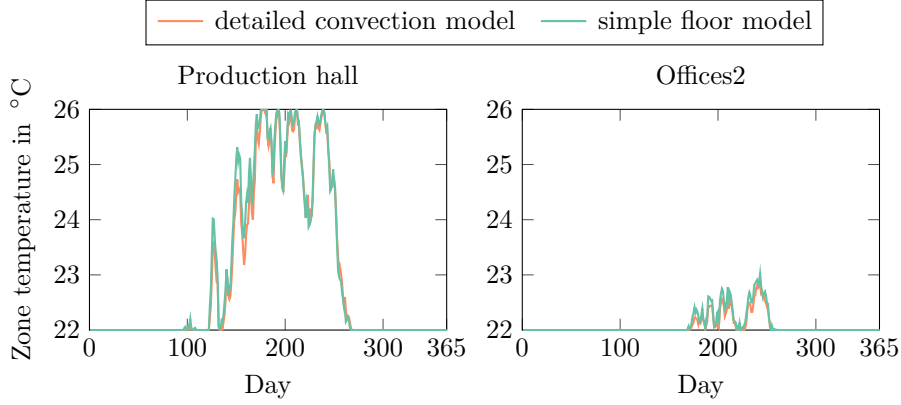


Figure 25: Daily average of zone temperatures for simple floor model.

lower RMSE values, meaning that the trend of heating and cooling demand shows lower deviation to the reference EnergyPlus simulation. Consequently the floor model has little influence on the overall results of the simulation. Especially for time critical tasks simplifying the floor model is recommended.

Table 9: Deviation of simple floor model to detailed convection model.

Difference to detailed convection model	Cold warehouse	Ware-house	Production hall	Offices2
Heating demand		+0.18%	-0.80%	-0.92%
Cooling demand	+2.15%	-0.27%	+82.38%	
Combined heating and cooling demand	+2.15%	+0.01%	+0.27%	-0.92%
RMSE	0.31	0.04	1.00	0.89
MBE	-0.31	0.03	-0.16	-0.10

7.4 Lumped walls

As a next step all walls are lumped into one equivalent wall. The equations for the lumped model are derived from summing up the individual equations and therefore are similar to those of the Dymola model. The transient energy balances merge to:

$$\sum_i C_{w,i} \frac{dT_w}{dt} = \dot{q}_{wi} + \dot{q}_{we} \quad (65)$$

With T_w as the wall temperature, \dot{q}_{wi} and \dot{q}_{we} as the heat flux between the wall node and the internal respectively external surface.

$$\dot{q}_{wi} = \frac{T_{wi} - T_w}{R_{wi}} \quad (66)$$

$$\dot{q}_{we} = \frac{T_{we} - T_w}{R_{we}} \quad (67)$$

Here T_{wi} is the interior wall surface temperature and T_{we} the exterior wall surface temperature. R_{wi} and R_{we} are the two conductive resistances of the wall. The equation for this resistances is derived from summing up each $\dot{q}_{wi,i}$, respectively $\dot{q}_{we,i}$. The conductive resistances of all walls could be considered a parallel circuit and therefore the equivalent conductive resistance can be calculated via

$$R_{ges} = \frac{1}{\sum_n \frac{1}{R_n}} : \quad (68)$$

$$\frac{1}{R_{wi}} = \sum_i \frac{1}{R_{wi,i}} \quad (69)$$

$$\frac{1}{R_{we}} = \sum_i \frac{1}{R_{we,i}} \quad (70)$$

The heat flux between the wall node and the internal and external surface is calculated as follows:

$$\dot{q}_{wi} = \dot{q}_i + \sum_i \dot{q}_{sgw,i} \quad (71)$$

$$\dot{q}_{we} = \dot{q}_e + \sum_i \dot{q}_{s,i} \quad (72)$$

Additional energy balances combine the heat flow rate on the internal/external surface with the solar contributions:

$$\dot{q}_i = \frac{T_i - T_{wi}}{R_i} \quad (73)$$

$$\dot{q}_e = (T_{ext} - T_{we}) UA_e \quad (74)$$

Where R_i is the equivalent internal convective resistance and $\frac{1}{UA_e}$ the equivalent external convective resistance. The term UA_e is chosen over R_e to avoid division through zero.

$$R_i = \frac{1}{h_i \sum_i A_{w,i}} \quad (75)$$

$$h_i = \frac{\sum_i h_{i,i} A_{w,i}}{\sum_i A_{w,i}} \quad (76)$$

$$UA_e = \sum_i h_{co,i} A_{w,i} \quad (77)$$

$$T_{ext} = \frac{\sum_i h_{co,i} A_{w,i} T_{e,i}}{UA_e} \quad (78)$$

Here h_i is the equivalent convection coefficient for the lumped wall. T_{ext} is an equivalent exterior temperature. It is calculated similar to VDI 6007 [32].

The following charts show the trends of the lumped model and the lumped model with a smaller effective thermal capacity (for the wall). According to Antonopoulos & Koronaki [33] the summation of all thermal capacities leads to incorrect results because the heat storage in walls is different when lumped together and not distributed. Antonopoulos & Koronaki determined, what they call effective thermal capacity C_{eff} by inverse modeling. They conclude that the effective thermal capacity is always smaller than the lumped capacity $\sum_i C_{w,i}$.

For an insulated house C_{eff} is about 2.2–3.1 times smaller than the overall lumped capacity [33]. Here the effective thermal capacity was set to one-third of the overall lumped capacity.

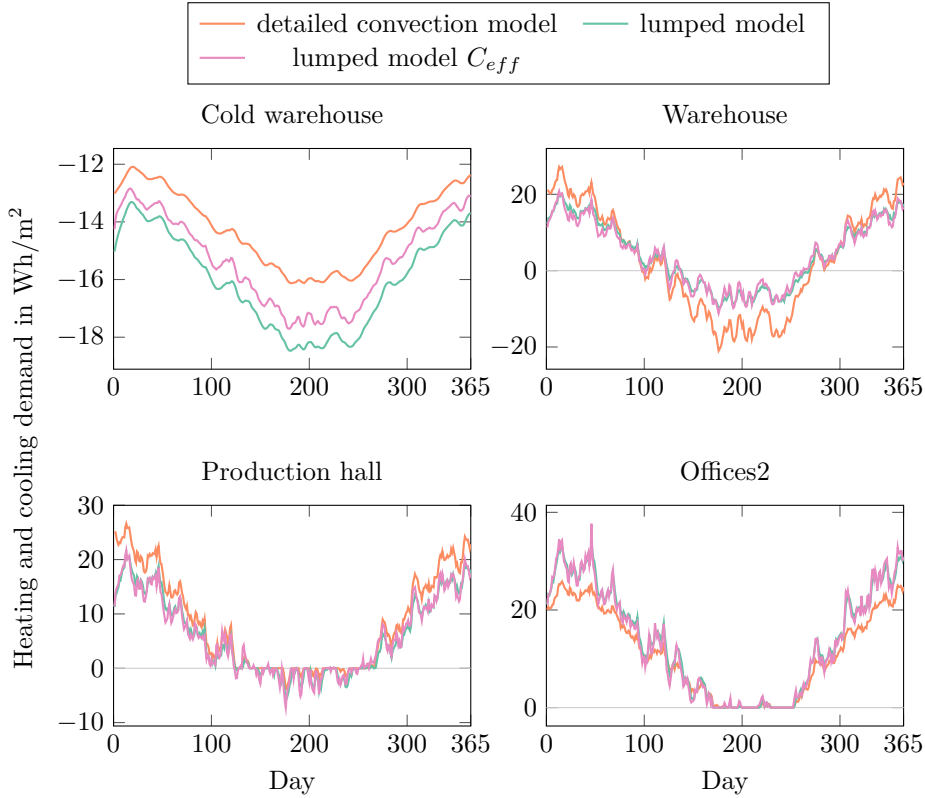


Figure 26: Daily average of heating and cooling demand for lumped wall models.

In this section the trends of a lumped model and also a lumped model with C_{eff} are compared to the proposed Dymola model. A quick look at the heating and cooling demand of the lumped wall model (see figure 26) and the effective lumped wall model shows that the results are not very accurate. Even in the zone *cold warehouse* the deviation of cooling demand is about 8 to 13 % (see table 10). For zones exposed to wind and solar radiation the differences get substantially higher, ranging from about -60 to 257 %. We can see no clear trend. In some zones the heating demand for the lumped models is higher than

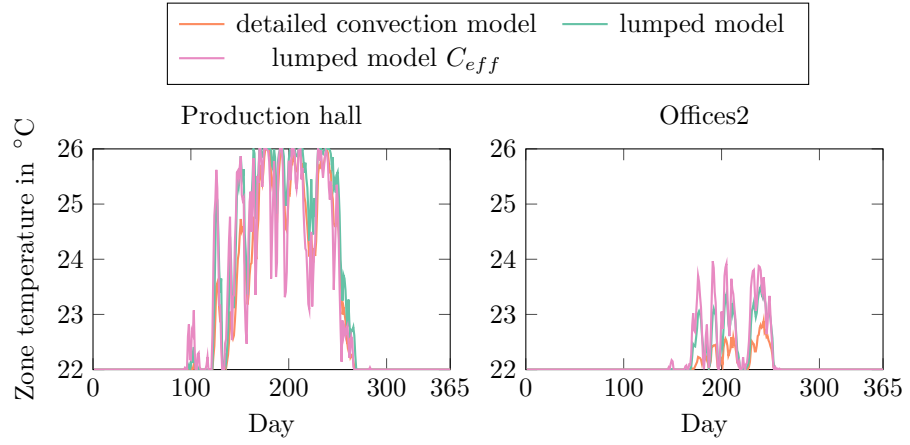


Figure 27: Daily average of zone temperatures for lumped wall models.

in the detailed convection model, in other zones it is smaller. The same is true for the cooling demand. Overall the C_{eff} model shows a lower bias but has a higher deviation than the lumped model.

The analysis of the zone air temperatures (see figure 27) shows that the lumped models lead to higher temperatures than the detailed convection model. However they show a similar dynamic and values compared to the reference simulation. To conclude, the lumped models are not very accurate but still can be used for rough estimations. Especially as the simulation times are reduced substantially. The concept of effective thermal capacity showed no real improvements over the lumped wall capacitances.

Table 10: Deviation of lumped models to the detailed convection model.

Difference to detailed convection model	Model	Cold warehouse	Ware- house	Production hall	Offices2
Heating demand	lumped c_{eff}		-16.15% -19.28%	-25.10% -24.53%	+22.05% +20.48%
Cooling demand	lumped c_{eff}	+12.85% +7.74%	-57.23% -59.26%	+257.28% +266.56%	
Combined heating and cooling demand	lumped c_{eff}	+12.85% +7.74%	-32.02% -34.72%	-21.48% -20.79%	+22.05% +20.48%
RMSE	lumped c_{eff}	1.86 1.13	5.16 5.53	3.15 3.39	3.41 3.67
MBE	lumped c_{eff}	-1.83 -1.10	1.48 1.34	-2.44 -2.40	2.47 2.30

7.5 Solar radiation

There is a plethora of simplified solar radiation models available and also a huge number of approaches on how to incorporate solar radiation into the model. For example Nielsen [20] only takes the solar radiation through windows into account. He furthermore splits the solar gains into a part directly hitting the interior wall surface and a second part directly absorbed by the internal air. Others take the solar radiation via the sol-air temperature into account.

Here solar radiation on an external wall is absorbed by the respective wall and solar radiation entering through windows is absorbed by the floor and the interior walls. The proposed model calculates the global solar radiation by adding the direct beam radiation, diffuse radiation and ground reflected radiation. Input for this model are measured normal direct radiation and diffuse radiation on the horizontal surface. The detailed model uses the Perez model for the calculation of the diffuse radiation part. The Liu & Jordan isotropic sky model [34] is often used in engineering calculations because it is the simplest (isotropic) sky model:

$$I_{d,n} = I_{d,h} \frac{1 + \cos(\beta)}{2} \quad (79)$$

A comparison between the more accurate Perez model and the Liu & Jordan model shows that the Liu & Jordan model overestimates the global solar radiation for a vertical wall orientated north by 12.3 %. For the other orientations it underestimates the global solar radiation (conservative model).

Table 11: Deviation of yearly total solar radiation of isotropic sky model to Perez model

Direction	Deviation in %
North	+12.30%
East	-5.97%
South	-8.19%
West	-0.88%

Comparing the heating and cooling demand (see figure 28) as well as the zone air temperature (see figure 29) there is virtually no difference between the anisotropic Perez model and the isotropic model (simple solar model). For comparison a third model without any solar radiation was simulated. As expected the omitted solar radiation leads to higher heating demands and lower cooling demands. Only in the zone *offices2* the omitted solar radiation leads to similar results compared to the models with solar radiation.

Looking at the zone air temperatures we see that the models incorporating solar radiation lead to very similar result, whereas the model with omitted solar radiation leads to substantially lower air temperatures. In the zone *production hall* the air temperature does not even increase in summer.

We conclude that the solar radiation has to be taken into account. The effect of choosing a simpler isotropic over a more complex model is negligible (note the low RMSE and MBE values in table 12). However zones with a higher share of walls exposed to solar radiation could be more sensible to an accurate modeling of solar radiation. As the Perez model only needs the extraterrestrial

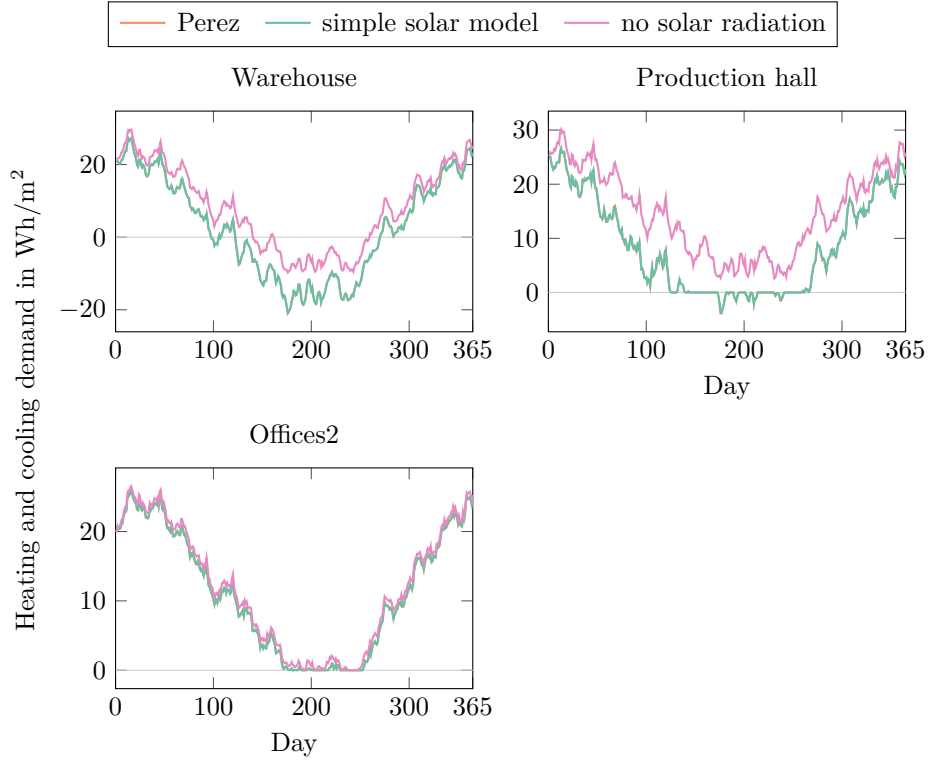


Figure 28: Daily average of heating and cooling demand for various solar radiation models.

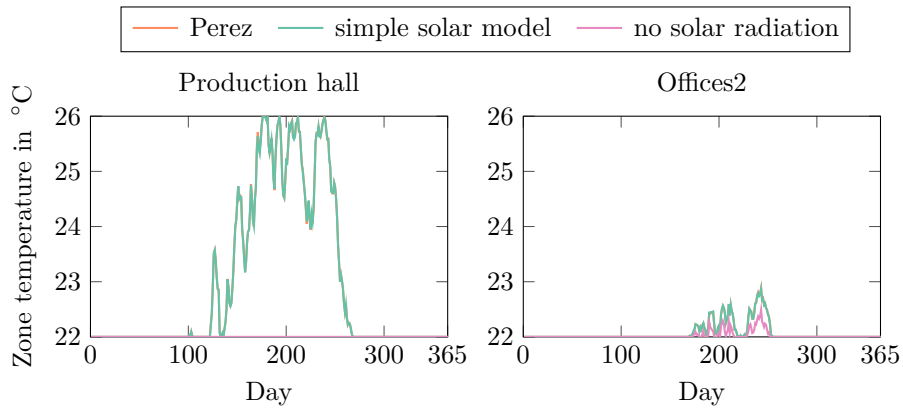


Figure 29: Daily average of zone temperatures for various solar radiation models.

irradiance as additional input (which is normally provided by the weather file) the Perez model is favored over the isotropic and quasi-isotropic models.

Table 12: Deviation of various solar models to the Perez model.

Difference to Perez model	Solar model	Ware- house	Production hall	Offices2
Heating demand	isotropic	+0.06%	+0.23%	+0.33%
	none	+33.10%	+72.49%	+7.11%
Cooling demand	isotropic	+0.28%	-5.15%	
	none	-61.19%	-100.00%	
Combined heating and cooling demand	isotropic	+0.14%	+0.16%	+0.33%
	none	-3.31%	+70.27%	+7.11%
RMSE	isotropic	0.08	0.09	0.07
	none	5.86	6.84	0.98
MBE	isotropic	-0.01	0.03	0.04
	none	5.33	6.32	0.80

7.6 Neglected thermal capacity of walls

This model is based on the presented model, however the thermal capacitance of every wall is set to zero. This reduces the system of differential equations for every wall to one simple equation. Looking at the heating and cooling demand charts (figure 30) we see that the reduced model basically follows the trend of the detailed model but with high deviations from this curve. Table 13 puts this trend into numbers. While the MBE is around zero, showing a good resemblance between detailed and simplified model, the RMSE shows high deviations. The thermal capacitance of the walls smooths the trend of heating and cooling demand. In the zone *cold warehouse* the deviations are very small because the walls of this zone are not exposed to wind and solar radiation. The other zones fluctuate greatly around the curve for the detailed convection model.

As the results of the heating and cooling demand for the neglected thermal wall-capacity model are usable, the results for the zone air temperature (see figure 31) are not as reliable. Especially in the zone *production hall* the temperature trends have no resemblance. In the zone *offices2* the trend of the air temperature shows reasonable results, because the heating and cooling demand shows little deviation to the detailed convection model.

Because of the very low bias error (see table 13) the results for the heating and cooling demand of the simplified model can be used. Especially if the curves are smoothed or processed afterwards they can be very useful for a first estimation.

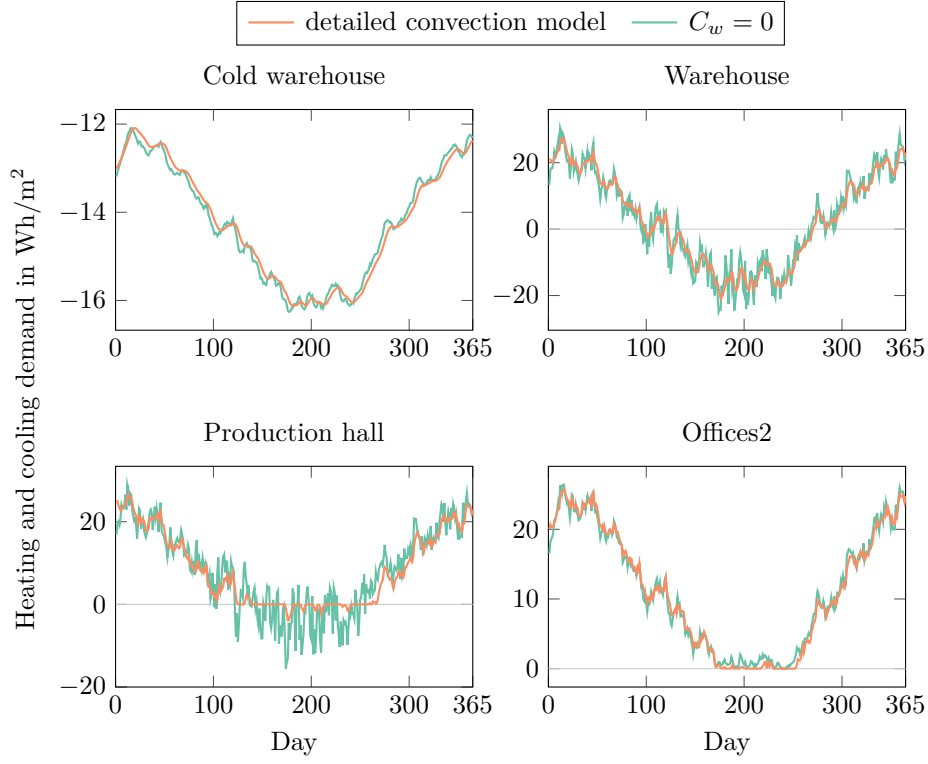


Figure 30: Daily average of heating and cooling demand for model neglecting C_w .

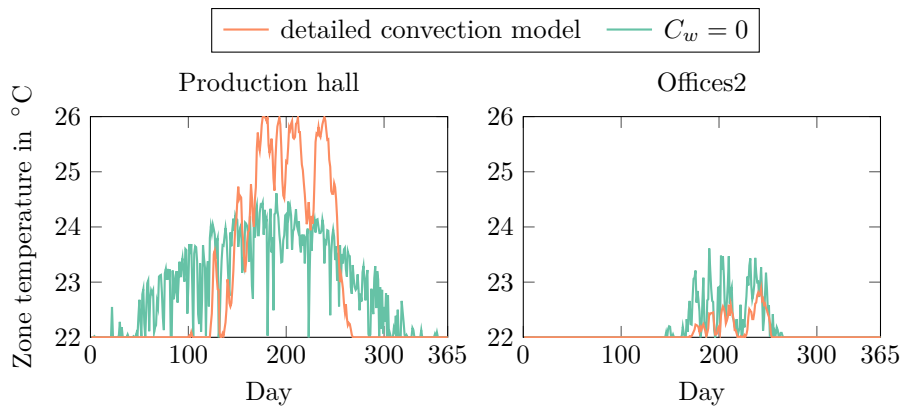


Figure 31: Daily average of zone temperatures for model neglecting C_w .

Table 13: Deviation of model neglecting C_w to detailed convection model.

Difference to detailed convection model	Cold warehouse	Ware-house	Production hall	Offices2
Heating demand		+13.69%	+29.04%	+1.46%
Cooling demand	+0.07%	+22.75%	+2350.77%	
Combined heating and cooling demand	+0.07%	+17.19%	+58.82%	-1.46%
RMSE	0.18	9.38	11.24	2.01
MBE	-0.01	-0.05	-0.13	0.16

7.7 Minimal model

The minimal model is the most basic model examined, incorporating only conduction through walls, windows and doors, infiltration, thermal capacity of indoor air and the solar radiation through windows. The heat transfer through walls is calculated via:

$$\dot{Q}_w = - \sum_i U_i A_i (T_i - T_{e,i}) - \sum_j U_j A_j (T_i - T_{ground}) - \sum_i qsgw_i \quad (80)$$

Not incorporated are the convection, the thermal capacity of the walls and the floor model with the thermal capacity of the floor. Models of such simple form are often used for early estimation of heating and cooling demand.

Comparing the reference EnergyPlus simulation to this basic model (see figure 32) one notices the very high deviations of heating and cooling demand. These deviations and also the RMSE and MBE (see table 14) are the highest encountered in this chapter. Only the temperature trend of the zone *offices2* (see figure 33) shows a good resemblance with the detailed EnergyPlus simulation. Overall this model overestimates heating and cooling demand. Although these simulations are used for a first estimation of energy demand they are magnitudes away from realistic or accurate values. Therefore the model with neglected thermal capacity of the walls is preferred over the minimal model. Note that the model with neglected thermal capacity of the walls needs to model convection, the minimal model does not.

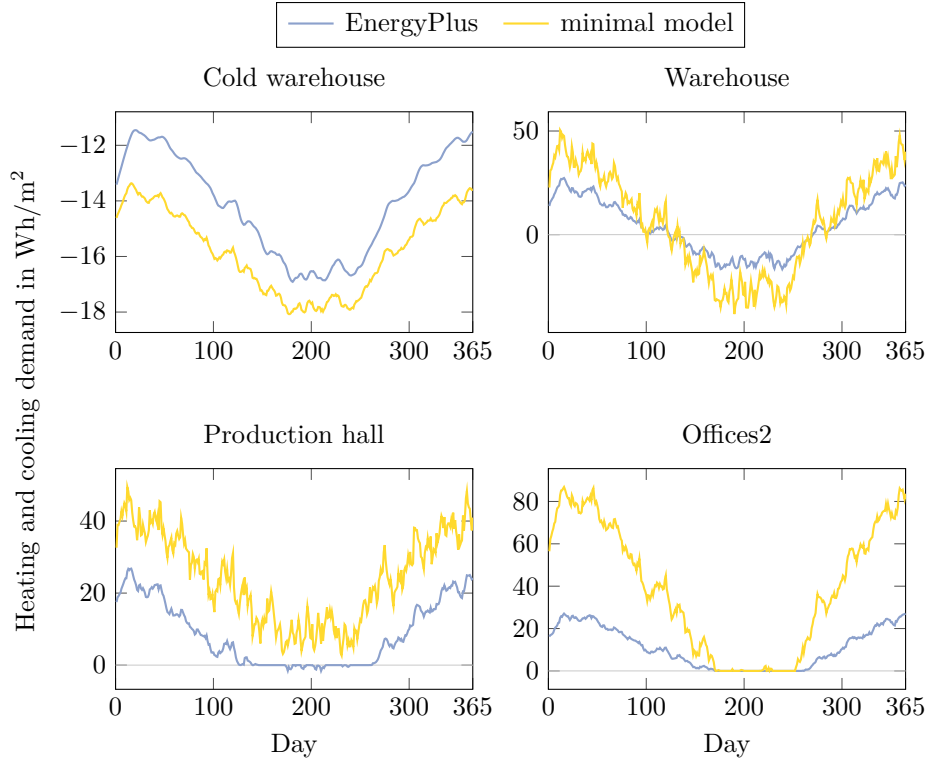


Figure 32: Daily average of heating and cooling demand for minimal model.

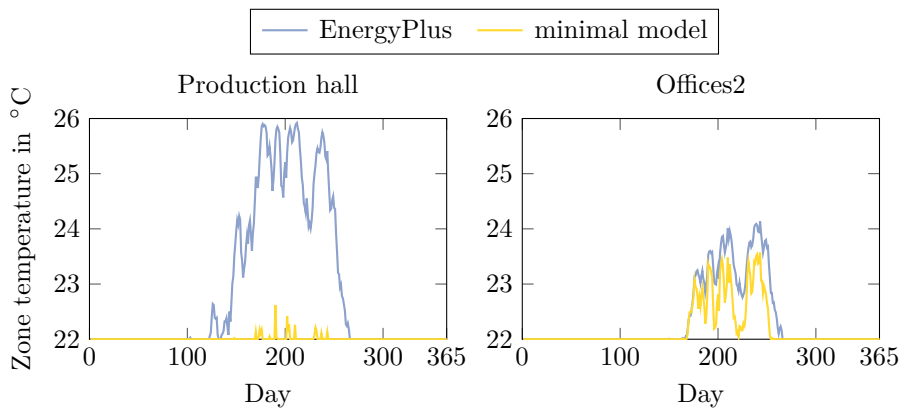


Figure 33: Daily average of zone temperatures for minimal model.

Table 14: Deviation of minimal model to detailed convection model.

Difference to detailed convection model	Cold warehouse	Ware-house	Production hall	Offices2
Heating demand		+84.90 %	+180.62 %	+258.76 %
Cooling demand	+12.13 %	+110.32 %	-100.00 %	
Combined heating and cooling demand	+12.13 %	+93.43 %	+178.91 %	+258.76 %
RMSE	1.76	12.86	17.15	34.73
MBE	1.71	11.11	15.74	27.84

7.8 Computation time

Figure 34 shows the computation time for the detailed convection model and the simplified models for each thermal zone. The simulation times for the different solar models are not shown because they are calculated externally and therefore have no influence on the simulation time.

The detailed convection model is the most sophisticated model and naturally requires the highest computation time. Using the simplified convection model the computation time is reduced by up to more than 10 times. The model with constant convection coefficients further reduces the computation time to 0.45 – 1.64 s. The simplified floor model requires nearly the same computation time as the detailed convection model except for the zone *offices2*. *Offices2* has two floors while all other zones have one floor and therefore the simulation time for *offices2* is drastically reduced. The lumped wall model, in which all walls are lumped into a single wall, shows very low computation times (as expected). The model with neglected thermal capacity of walls ($C_w = 0$) results in low computation times because the differential equations for the energy balance of each wall are reduced to scalar equations. The minimal model results in the lowest simulation times (0.36 – 0.55 s).

Table 15 lists the number of scalar equations for the proposed model and its simplifications for each thermal zone. Comparing the number of equations to computation times we see that there is no correlation between the number of equations and required computation time. Especially the equation of the convection coefficients (equation (28)) is computation heavy.

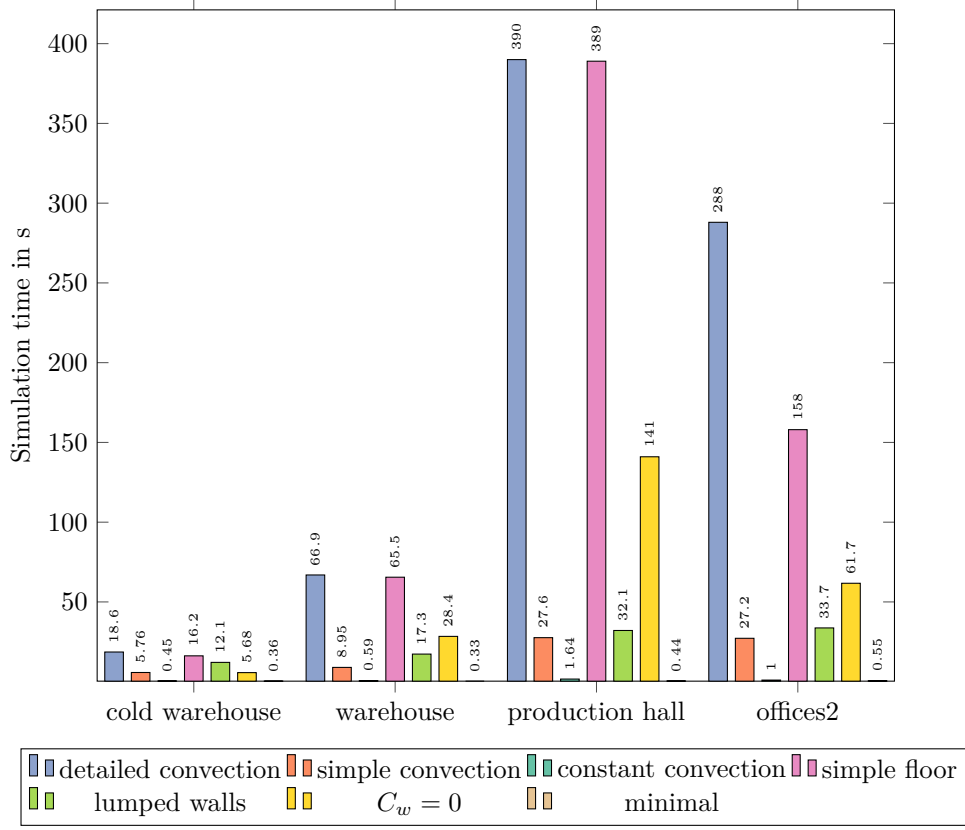


Figure 34: Simulation times for different models.

Table 15: Number of scalar equations.

Model	Cold warehouse	Ware-house	Production hall	Offices2
Number of walls	3	13	16	9
Number of floors	1	1	1	2
detailed convection	181	513	614	426
simple convection	181	473	565	397
constant convection	176	469	577	403
simple floor	170	501	602	403
lumped walls	162	410	484	359
$C_w = 0$	181	513	614	426
minimal	99	182	309	234

7.9 Verdict

One outcome of the analysis of simulation accuracy and computation time is that the required simulation time is not directly correlated with the model's accuracy. The presented detailed convection model has a very high accuracy, however it is also the most computation intensive model. The simple convection model has nearly the same accuracy but is about 3 to 14 times faster, depending on the zone's complexity. Also the lumped wall model requires roughly the same computation time as the simple convection model, however the lumped wall model lacks the simple convection model's accuracy. Nevertheless, as a rule of thumb, faster models are in general less accurate than more complex models. There is always a trade-off between accuracy and computation time. The detailed analysis of the different simplified models in this section will help to choose the right model for a specific application.

Furthermore two or more simplifications could be applied at once. For example the simple convection model could be combined with the simple floor model. The simple floor model in general would be suitable for most simplified models, because it does not effect the wall model or the convection model. Also walls with the same orientation could be lumped together (like in the lumped wall approach), however this simplification was not conducted because only one zone had two walls with the same orientation.

All in all, the simplified convection model seems to be the best choice for general applications due its accuracy and fast computation time. Also the model can first be validated by the detailed convection model in order to choose the right convection coefficients.

8 Conclusion and outlook

A simplified building simulation model based on the RC method was introduced. Compared to more detailed building simulation programs the proposed Dymola model has a plethora of advantages: First of all, the time needed for setting up the model and start the first simulation runs is lower. Also the proposed model requires less input parameters than detailed simulation programs. Therefore the proposed model can be applied in the earliest design phase and can help to choose ideal geometries or properties. Another advantage of the proposed model is its re-usability which yields a decrease of needed man-hours and cost. Advantageous, especially for scientific applications, is that one has full control over the model. Meaning that one can decide how to model a physical phenomenon and has control over numerical approximations. In terms of accuracy the proposed model shows little deviation to the detailed EnergyPlus simulation. The biggest deviation of total energy demand is as low as 4.36 %. Comparing the heating and cooling demands over a year the close resemblance of the results of the proposed model and the detailed EnergyPlus simulation is obvious. The simulation time for one zone is relatively low, ranging from 18.6 to 390 s depending on the complexity of a zone. If lower computation times are required or certain input parameters are unknown various simplifications can be made to the proposed model. These simplifications can have a major impact on accuracy and computation time. Therefore the right choice depends on the scope of application. In general the detailed convection model (proposed model) has the highest accuracy at the price of the highest computation time. The simple convection model has a up to ten times lower computation time while the accuracy is close to the detailed convection model. However the accuracy of the simple convection model is a bit of a mixed bag. Sometimes it is even (marginally) better than the detailed convection model, at other times the deviation to the EnergyPlus simulation is twice as high (but still very accurate). The simplified floor model showed very little deviation to the proposed model. As the simple floor model only concerns the floor and does not effect the wall or convection model it could easily be applied together with another simplification. Due time constraints two or more simplifications of the proposed model were not applied together. However these results would have been very interesting and can be subject to future evaluations. The model with lumped walls (all walls are lumped into a single fictive wall) has a mediocre accuracy and may be suitable for rough estimations in time critical applications. Again a combination of the lumped wall model with the simple floor model or the simple convection model would have been of great interest. For the examined zones the accuracy of the used diffuse solar radiation model has a minor impact on accuracy of heating and cooling demand and zone air temperature. However not taking solar radiation into account at all leads to higher heating demands and lower cooling demands. Therefore the heating and cooling demands have a positive bias and fairly high deviations. It is not important which solar model is chosen as long as solar radiation is taken into account at all. The results of the model with neglected thermal capacity of walls are of special interest. The curve of the heating and cooling demand follows basically the trend of the proposed model (low MBE) but with very high deviations to it (very high RMSE). The results of the heating and cooling demand may be usable if these results are post-processed afterwards by smoothing the curve. The last simplified model

is called the minimal model. This model only takes conduction, solar radiation through windows and infiltration into account. As there is no complex convection coefficient calculation necessary nor the differential equations for the walls and floors this model has the lowest computation times, which are less than one second for every zone. However the accuracy is the worst of all the simplified models. The model with constant convection coefficients can reach considerably better results (if the convection coefficient is properly chosen) with similar computation time. Again a model containing constant convection coefficients for indoor and higher constant convection coefficients for exterior convection could lead to results with decent accuracy and very low computation time.

To sum up, the proposed model shows a very good accuracy with reasonable computation time. Therefore it is recommended over the other models. However if computation time is crucial one of the simplified models could be used. Especially the simple convection model seems to be a very good compromise between accuracy and computation time.

As the convection model has the biggest influence on the computation time a comparison between different convection models (not only the MoWiTT model) would be very insightful. [21] gives a detailed overview of a plethora of different models for the calculation of the convection coefficients.

As the proposed model's wall model discretized the wall into one node (one capacitance) a discretization into two or more nodes would be interesting, as models with higher order are more accurate but on the other hand have higher computation time. Due to time constraints higher order models could not be tested. However they require no additional information and could therefore easily be implemented. [2] tests wall models of first, second and third order and comes to the conclusion that the second order model achieves very good results with reasonable computation effort.

To sum up, new technologies for energy efficient buildings require more flexible simulation models as well as short computation times. Simple and flexible thermal building simulation models, like the one presented, help to fulfill this need. The proposed model is easy to use, adapt-, extend- and simplifyable while still providing a very good accuracy at low computational costs.

References

- [1] D. Ürge-Vorsatz, L. F. Cabeza, S. Serrano, C. Barreneche, and K. Petrichenko. Heating and cooling energy trends and drivers in buildings. *Renewable and Sustainable Energy Reviews*, 41:85–98, 2015.
- [2] M. De Rosa, V. Bianco, F. Scarpa, and L. A. Tagliafico. Impact of wall discretization on the modeling of heating/cooling energy consumption of residential buildings. *Energy Efficiency*, 1-14, 2015.
- [3] G. Arcangeli. Advanced Tools for Building Simulation: Energy and Air-flow.
- [4] L. Mazzarella, and M. Pasini. Building energy simulation and object-oriented modelling: Review and reflections upon achieved results and further developments. In *Proceedings of the International IBPSA Conference (IBPSA)*, pages 638–645, Glasgow, Scotland, 2009.
- [5] M.S. Al-Homoud. Computer-aided building energy analysis techniques. *Building and Environment*, 36:421–433, 2001.
- [6] T. Hong, S. K. Chou, and T. Y. Bong. Building simulation: an overview of developments and information sources. *Building and Environment*, 35:347–361, 2000.
- [7] A. Fouquier, S. Robert, F. Suard, L. Stéphan, and A. Jay. State of the art in building modelling and energy performances prediction: A review. *Renewable and Sustainable Energy Reviews*, 23:272–288, 2013.
- [8] N. Fumo. A review on the basics of building energy estimation. *Renewable and Sustainable Energy Reviews*, 31:53–60, 2014.
- [9] H.-x. Zhao, and F. Magoulès. A review on the prediction of building energy consumption. *Renewable and Sustainable Energy Reviews*, 16:3586–3592, 2012.
- [10] M. Wetter. *Building performance simulation for design and operation*, volume 1, chapter A view on future building system modeling and simulation, pages 481–504. Spon Press, Oxon, 2011.
- [11] M. Wetter, and C. Haugstetter. Modelica vs TRNSYS - A comparison between an equation-based and a procedural modeling language for building energy simulation.
- [12] G. Fraisse, C. Viardot, O. Lafabrie and G. Achard. Development of a simplified and accurate building model based on electrical analogy. *Energy and Buildings*, 34:1017-1031, 2002.
- [13] R. Kramer, J. van Schijndel, and H. Schellen. Simplified thermal and hygric building models: A literature review. *Frontiers of Architectural Research*, 1:318–325, 2012.
- [14] G. Parnis. Building Thermal Modelling Using Electric Circuit Simulation. Master’s thesis, UNSW Sydney, 2012.

- [15] O. T. Ogunsola, and L. Song. In *Proceedings of the ASME 2012 International Mechanical Engineering Congress & Exposition*, volume 7, pages 735–744, 2012.
- [16] DOE, U. S. EnergyPlus engineering reference. *The Reference to EnergyPlus Calculations*, 2014.
- [17] LBNL, EnergyPlus. EnergyPlus Documentation: Getting Started with EnergyPlus. *Auxiliary EnergyPlus Programs*, 2013.
- [18] M. De Rosa, V. Bianco, F. Scarpa, and L. A. Tagliafico. Heating and cooling building energy demand evaluation; a simplified model and a modified degree days approach. *Applied Energy*, 128:217–229, 2014.
- [19] J. Crabb, N. Murdoch, and J. Pennman. A simplified thermal response model. *Building Services Engineering Research and Technology*, 8:13–19, 1987.
- [20] T. R. Nielsen. Simple tool to evaluate energy demand and indoor environment in the early stages of building design. *Solar Energy*, 78:73–83, 2005.
- [21] J. A. Palyvos. A survey of wind convection coefficient correlations for building envelope energy systems’ modeling. *Applied Thermal Energy*, 28:801–808, 2008.
- [22] A. Buonomano, and A. Palombo. Building energy performance analysis by an in-house developed dynamic simulation code: An investigation for different case studies. *Applied Energy*, 113:788–807, 2014.
- [23] M. Yazdanian, and J. H. Klems. Measurement of the Exterior Convective Film Coefficient for Windows in Low-Rise Buildings. In *ASHRAE transactions*, volume 100, pages 1–19, 1994.
- [24] S. A. Kalogirou. *Solar energy engineering: processes and systems*. Academic Press, Oxford, 2. edition, 2014.
- [25] D. Wlodarczyk, and H. Nowak. Statistical analysis of solar radiation models onto inclined planes for climatic conditions of Lower Silesia in Poland. *Archives of civil and mechanical engineering*, 9:127–144, 2009.
- [26] VDI 6007 Blatt 3: Berechnung des instationären thermischen Verhaltens von Räumen und Gebäuden - Modell der solaren Einstrahlung, 2012.
- [27] B. Y. H. Liu, and R. C. Jordan, The long-term average performance of flat-plate solar-energy collectors: with design data for the US, its outlying possessions and Canada. *Solar Energy*, 7:53–74, 1963.
- [28] R. Perez, R. Stewart, R. Seals, and T. Guertin. *The development and verification of the Perez diffuse radiation model*. No. SAND-88-7030. Sandia National Labs., Albuquerque, NM (USA); State Univ. of New York, Albany (USA). Atmospheric Sciences Research Center, 1988.
- [29] F. Kasten, and A. T. Young. Revised optical air mass tables and approximation formula. *Applied optics*, 28:4735–4738, 1989.

- [30] R. Perez, P. Ineichen, R. Seals, J. Michalsky, and R. Stewart. Modeling daylight availability and irradiance components from direct and global irradiance. *Solar Energy*, 44,271–289, 1990
- [31] M. de Wit. *HAMBASE: Heat Air and Moisture Model for Building and Systems Evaluation*. Technische Universiteit Eindhoven, Eindhoven, Netherlands, 2006.
- [32] VDI 6007 Blatt 1: Berechnung des instationären thermischen Verhaltens von Räumen und Gebäuden - Raummodell, 2012.
- [33] K. A. Antonopoulos, and E. Koronaki. Apparent and effective thermal capacitance of buildings. *Energy*, 23:183–192, 1998.
- [34] B. Y. H. Liu, and R. C. Jordan. The interrelationship and characteristic distribution of direct, diffuse and total solar radiation. *Solar Energy*, 4:1–19, 1960.

List of Figures

1	Thermal phenomena in building simulations.	2
2	Decision costs and their impact on the performance of buildings.	4
3	Overview of thermodynamic building simulation methods.	5
4	Overview of nodal approach methods.	6
5	Electrical analogy of conduction through a wall layer.	10
6	Wall model in EnergyPlus.	12
7	Building, view from north.	15
8	Building, view from south.	16
9	Schematic view of heat transfers in a zone.	17
10	Wall model in electric analogy.	19
11	Equation of time.	24
12	Daily path of the sun across the sky from sunrise to sunset.	25
13	Declination of the sun.	25
14	Calculation of the solar azimuth angle (z).	27
15	Heating and cooling demand for different initial values.	32
16	Wall temperature for different initial values.	33
17	Heating and cooling demand with and without dummy period.	33
18	Daily average of heating and cooling demand for detailed convection model.	36
19	Daily average of zone temperatures for detailed convection model.	37
20	Daily average of heating and cooling demand for simple convection model.	39
21	Daily average of zone temperatures for simple convection model.	40
22	Daily average of heating and cooling demand for various convection coefficients.	42
23	Daily average of zone temperatures for various convection coefficients.	42
24	Daily average of heating and cooling demand for simple floor model.	44
25	Daily average of zone temperatures for simple floor model.	45
26	Daily average of heating and cooling demand for lumped wall models.	47
27	Daily average of zone temperatures for lumped wall models.	48
28	Daily average of heating and cooling demand for various solar radiation models.	51
29	Daily average of zone temperatures for various solar radiation models.	51
30	Daily average of heating and cooling demand for model neglecting C_w	53
31	Daily average of zone temperatures for model neglecting C_w	53
32	Daily average of heating and cooling demand for minimal model.	55
33	Daily average of zone temperatures for minimal model.	55
34	Simulation times for different models.	57

List of Tables

1	Thermal-electric analogy.	10
2	Overview of zone characteristics.	16
3	Constants for calculation of convection coefficients	22
4	Discrete sky clearness categories.	29
5	Perez model coefficients	30
6	Deviation of detailed convection model to the reference simulation.	37
7	Deviation of simple convection model to the reference simulation.	41
8	Deviation of various convection coefficients to the reference simulation.	43
9	Deviation of simple floor model to detailed convection model.	45
10	Deviation of lumped models to the detailed convection model.	49
11	Deviation of yearly total solar radiation of isotropic sky model to Perez model	50
12	Deviation of various solar models to the Perez model.	52
13	Deviation of model neglecting C_w to detailed convection model.	54
14	Deviation of minimal model to detailed convection model.	56
15	Number of scalar equations.	57

A Modelica code for the detailed convection model

```
1 model offices2_detailed_convection_model
2   "Model for multiple walls, contains RC model"
3
4   //This is the wall model. Every wall has a area A, a thickness d
5   //as well as a thermal conduction resistance R and thermal
6   //capacitance C for every wall layer.
7   //The wall model can calculate the overall thermal conductance
8   //and thermal capacity.
9   RC5 W1(A=20.93, d=0.56, R1=0.1579, C1=7.992*10^5, R2=0.158, C2=0,
10      R3=0.00001667, C3=3768, R4=2.857, C4=4200, R5=0.00001667,
11      C5=3768);
12   RC2 W2(A=32.46, d=0.33, R1=0.5102, C1=2.875*10^5, R2=2, C2=3480);
13   RC5 W3(A=86.51, d=0.582, R1=0.1579, C1=7.992*10^5, R2=0.18, C2=0,
14      R3=0.00001667, C3=3768, R4=2.857, C4=4200, R5=0.00001667,
15      C5=3768);
16   RC3 W4(A=172.93, d=0.25, R1=0.1224, C1=69*10^4, R2=0.06842,
17      C2=3.4632*10^5, R3=0.1224, C3=6.9*10^4);
18   RC1 W5(A=38.96, d=0.3, R1=0.1579, C1=7.992*10^5);
19   RC3 W6(A=131.97, d=0.25, R1=0.1224, C1=6.9*10^4, R2=0.06842,
20      C2=3.4632*10^5, R3=0.1224, C3=6.9*10^4);
21   RC1 W7(A=110.79, d=0.3, R1=0.1579, C1=7.992*10^5);
22   RC1 W8(A=10.29, d=0.01, R1=0.01667, C1=8000);
23   RC1 W9(A=785.1, d=0.4, R1=0.2105, C1=1.0656*10^6);
24   RC9 W10(A=697.08, d=0.653, R1=0.02, C1=4*10^4, R2=0.04286,
25      C2=1.296*10^5, R3=0.8, C3=1680, R4=0.004348, C4=1185,
26      R5=0.1143, C5=1.44*10^5, R6=0.1842, C6=9.324*10^5,
27      R7=0.00001667, C7=3768, R8=2.857, C8=4200,
28      R9=0.00001667, C9=3768);
29   RC9 W11(A=88.02, d=0.79, R1=0.04286, C1=1.296*10^5, R2=0.8,
30      C2=1680, R3=0.004348, C3=1185, R4=0.1143, C4=1.44*10^5,
31      R5=0.1842, C5=9.324*10^5, R6=0.157, C6=0, R7=0.00001667,
32      C7=3768, R8=2.857, C8=4200, R9=0.00001667, C9=3768);
33   //The last two (W10 and W11) are floors.
34
35
36   parameter Integer n(min=1)=9; //number of walls and ceilings
37   parameter Integer n_floor=2; //number of floors
38
39   Modelica.Blocks.Sources.CombiTimeTable temp(
40     tableOnFile=true,
41     fileName="C:/Dropbox/My Dropbox/master-arbeit/dymola/temp_sek.txt",
42     columns=2:17,
43     tableName="temp",
44     startTime=0); //loads ambient temperature and temperature of
45     //adjacent zones from a .txt file
46
47   Modelica.Blocks.Sources.CombiTimeTable sun(
48     tableOnFile=true,
49     fileName="C:/Dropbox/My Dropbox/master-arbeit/dymola/sun_sek_perez.txt",
50     columns=2:8,
51     tableName="sun",
52     startTime=0); //loads solar radiation, wind-speed and
53     //-direction from a .txt file
54
55
56   Modelica.SIunits.Temp_K Ti(start=295.15); //a start temperature
57   //has to be assigned for the indoor zone air temperature
```



```

58 Modelica.SIunits.Temp_K Tw[n];
59 Modelica.SIunits.Temp_K Twi[n];
60 Modelica.SIunits.Temp_K Twe[n];
61 Modelica.SIunits.Temp_K Twf[n_floor];
62 Modelica.SIunits.Temp_K Twif[n_floor];
63 Modelica.SIunits.Temp_K T_ground[n_floor]=fill(273.15+17,n_floor);
64 Modelica.SIunits.Temp_K Te[n]; //exterior temperatures
65
66 Modelica.SIunits.HeatCapacity Ci; //thermal capacity of indoor air
67 Modelica.SIunits.HeatCapacity Cw[n]; //thermal capacity of walls
68 Modelica.SIunits.HeatCapacity Cwf[n_floor]; //thermal capacity of walls
69
70 Modelica.SIunits.HeatFlowRate qwi[n];
71 Modelica.SIunits.HeatFlowRate qwe[n];
72 Modelica.SIunits.HeatFlowRate qwef[n_floor];
73 Modelica.SIunits.HeatFlowRate qwif[n_floor];
74
75 Modelica.SIunits.ThermalResistance Rwi[n];
76 Modelica.SIunits.ThermalResistance Rwe[n];
77 Modelica.SIunits.ThermalResistance RwiA[n];
78 Modelica.SIunits.ThermalResistance RweA[n];
79
80 Modelica.SIunits.ThermalResistance Rwif[n_floor];
81 Modelica.SIunits.ThermalResistance Rwef[n_floor];
82 Modelica.SIunits.ThermalResistance RwifA[n_floor];
83 Modelica.SIunits.ThermalResistance RwefA[n_floor];
84
85 Modelica.SIunits.ThermalConductance Ke[n];
86 //Ke is used instead of Re to avoid divison through zero
87 Modelica.SIunits.ThermalResistance Ri[n];
88 Modelica.SIunits.ThermalResistance Rif[n_floor];
89
90 Modelica.SIunits.HeatFlowRate qsg[n];
91 Modelica.SIunits.HeatFlowRate qsgw[n];
92 Modelica.SIunits.HeatFlowRate qsgf[n_floor];
93 Modelica.SIunits.HeatFlowRate qs[n];
94
95 Real alphaw[n];
96 Real alphaf=0.7;
97
98 Modelica.SIunits.HeatFlowRate qi[n];
99 Modelica.SIunits.HeatFlowRate qe[n];
100 Modelica.SIunits.HeatFlowRate qi_floor[n_floor];
101
102 Modelica.SIunits.SurfaceCoefficientOfHeatTransfer htot[n];
103 Real north; //variables for convection coefficient
104 Real east; //calculation
105 Real south;
106 Real west;
107 Real horizontal;
108 constant Real Ct=0.84;
109 constant Real aww=3.26;
110 constant Real alw=3.55;
111 constant Real bww=0.89;
112 constant Real blw=0.617;
113
114 Modelica.SIunits.Area Sw[n];
115 Modelica.SIunits.Area Swf[n_floor];
116 Modelica.SIunits.Area Swin[n];
117
118 Modelica.SIunits.DensityOfHeatFlowRate I[n];
119 Real tau[n];

```

```

120 Modelica.SIunits.Volume V=3297.41; //zone volume
121 Real n_inf(unit="1/s")=0.1/3600; //air-change rate
122
123
124 Modelica.SIunits.SurfaceCoefficientOfHeatTransfer hi[n];
125 //convection coefficient wall - interior side
126 Modelica.SIunits.SurfaceCoefficientOfHeatTransfer hif[n_floor];
127 //convection coefficient floor
128 Modelica.SIunits.SurfaceCoefficientOfHeatTransfer h_conv_nc[n];
129 //convection coefficient - natural convection term
130 Modelica.SIunits.SurfaceCoefficientOfHeatTransfer h_conv_fc[n];
131 //convection coefficient - forced convection term
132
133 parameter Modelica.SIunits.HeatFlowRate L=0; //internal gains
134
135 Modelica.SIunits.HeatFlowRate HC; //heating cooling demand
136
137 constant Modelica.SIunits.Density rho_air=1.204;
138 constant Modelica.SIunits.SpecificHeatCapacityAtConstantPressure cp_air=1005;
139
140 Modelica.SIunits.HeatFlowRate Q_inf; //heat flux infiltration
141 Modelica.SIunits.HeatFlowRate Q_w; //heat flux through walls
142 Modelica.SIunits.HeatFlowRate Q_win; //heat flux through windows and doors
143
144 constant Modelica.SIunits.ThermalConductance U_tuer=0.875;
145 parameter Modelica.SIunits.Area A_tuer=0;
146
147 constant Real U_tuer_aussentuer_glass(unit="W/(m2.K)")=1.7;
148 constant Real U_tuer_innentuer_glass(unit="W/(m2.K)")=3.504;
149 parameter Modelica.SIunits.Area A_tuer_aussentuer_glass=6.6;
150 parameter Modelica.SIunits.Area A_tuer_innentuer_glass=0;
151
152 constant Real U_fenster2(unit="W/(m2.K)")=1.4;
153 constant Real U_fenster3(unit="W/(m2.K)")=0.8;
154 parameter Modelica.SIunits.Area A_fenster2=11.2;
155 parameter Modelica.SIunits.Area A_fenster3=32.48;
156
157
158 initial equation
159   for i in 1:n loop
160     Tw[i]=(Te[i]/RweA[i]+Ti/RwiA[i])/(1/RweA[i]+1/RwiA[i]);
161   end for;
162
163   for i in 1:n_floor loop
164     Twf[i]=(T_ground[i]/RwefA[i]+Ti/RwifA[i])/(1/RwefA[i]+1/RwifA[i]);
165   end for;
166   //the initial equations estimate the wall temperatures
167   //for the start of the simulation
168
169
170 equation
171   Cw={W1.Cw, W2.Cw, W3.Cw, W4.Cw, W5.Cw, W6.Cw, W7.Cw, W8.Cw, W9.Cw};
172   Cwf={W10.Cw, W11.Cw};
173   //creates vectors with the thermal capacity of each wall, ceiling and floor
174
175   //conductive and convective resistances per square-meter,
176   //here they are calculated by hand
177   RwiA={0.1474, 0.3367, 0.1532, 0.1466, 0.079, 0.1466, 0.079, 0.0083, 0.1053};
178   RweA={3.0257, 2.1735, 3.0418, 0.1666, 0.079, 0.1666, 0.079, 0.0083, 0.1053};
179   RwifA={1.0476, 1.0741};
180   RwefA={2.9752, 3.0856};
181

```

```

182 //conductive and convective resistances per wall
183 for i in 1:n loop
184     Rwi[i]=RwiA[i]/Sw[i];
185     Rwe[i]=RweA[i]/Sw[i];
186 end for;
187 for j in 1:n_floor loop
188     Rwif[j]=RwifA[j]/Swf[j];
189     Rwef[j]=RwefA[j]/Swf[j];
190 end for;
191
192 alphaw={0.35, 0.7, 0.35, 0.6, 0.6, 0.6, 0.6, 0.7, 0.6};
193 tau={0.75, 0.6, 0.6, 0, 0, 0, 0, 0, 0};
194 //input of solar absorbance and glass transmission coefficient
195
196 Sw={W1.A, W2.A, W3.A, W4.A, W5.A, W6.A, W7.A, W8.A, W9.A};
197 Swf={W10.A, W11.A};
198 Swin={11.2, 21.84+6.6, 10.64, 0, 0, 0, 0, 0, 0};
199 //input of wall, floor and window areas
200
201 I={sun.y[2], sun.y[4], sun.y[5], 0, 0, 0, 0, 0, 0};
202 //input of solar radiation onto wall
203
204 Te={temp.y[1], temp.y[1], temp.y[1], temp.y[2], temp.y[5], temp.y[8],
205     temp.y[3], temp.y[13], temp.y[14]};
206 //input of exterior wall temperatures
207
208 Ci*der(Ti)=HC+L+Q_inf+Q_w+Q_win;
209
210 Ci=rho_air*V*cp_air;
211
212 Q_inf=(rho_air*cp_air*V*n_inf)*(temp.y[1]-Ti);
213
214 //calculation procedure for forced convection term:
215 if sun.y[6]>90 and sun.y[6]<270 then
216     north=alw*sun.y[7]^blw;
217 else
218     north=aww*sun.y[7]^bww;
219 end if;
220 if sun.y[6]>0 and sun.y[6]<180 then
221     east=aww*sun.y[7]^bww;
222 else
223     east=alw*sun.y[7]^blw;
224 end if;
225 if sun.y[6]>90 and sun.y[6]<270 then
226     south=aww*sun.y[7]^bww;
227 else
228     south=alw*sun.y[7]^blw;
229 end if;
230 if sun.y[6]>0 and sun.y[6]<180 then
231     west=alw*sun.y[7]^blw;
232 else
233     west=aww*sun.y[7]^bww;
234 end if;
235 horizontal=alw*sun.y[7]^blw;
236 h_conv_fc={north, south, west, 0, 0, 0, 0, 0, 0};
237
238 //calculation of convection coefficients (interior and exterior)
239 for k in 1:n loop
240     h_conv_nc[k]= 3+Ct*abs(Te[k] - Twe[k])^(1/3);
241     hi[k]= 3+Ct*abs(Twi[k]-Ti)^(1/3);
242     htot[k]=sqrt(h_conv_nc[k]^2+h_conv_fc[k]^2);

```

```

244 end for;
245 for k in 1:n_floor loop
246     hif[k]= 3+Ct*abs(Twif[k]-Ti)^(1/3);
247 end for;
248
249 //energy balance wall
250 for j in 1:n loop
251     der(Tw[j])= (qwi[j] + qwe[j])/Cw[j];
252     qwi[j]= (Twi[j] - Tw[j])/Rwi[j];
253     qwe[j]= (Twe[j] - Tw[j])/Rwe[j];
254     qwi[j]= qi[j] + qsgw[j]; //heat balance interior wall surface
255     qwe[j]= qe[j] + qs[j]; //heat balance exterior wall surface
256
257     qi[j]= (Ti - Twi[j])/Ri[j];
258     qe[j]= (Te[j] - Twe[j])*Ke[j];
259
260     //Re[j]= 1/(htot[j]*Sw[j]);
261     Ke[j]= (htot[j]*Sw[j]);
262     Ri[j]= 1/(hi[j]*Sw[j]);
263 end for;
264
265 //energy balance floor
266 for k in 1:n_floor loop
267     der(Twf[k])= (qwif[k] + qwef[k])/Cwf[k];
268     qwif[k]= (Twif[k] - Twf[k])/Rwif[k];
269     qwef[k]= (T_ground[k] - Twf[k])/Rwef[k];
270     qwif[k]= qi_floor[k] + qsgf[k]; //heat balance interior floor surface
271
272     qi_floor[k]= (Ti - Twif[k])/Rif[k];
273
274     Rif[k]= 1/(hif[k]*Swf[k]);
275 end for;
276
277
278 Q_w=-sum(qi)-sum(qwif);
279
280
281 Q_win=(temp.y[1]-Ti)*(U_tuer_aussentuer_glass*A_tuer_aussentuer_glass+
282 U_fenster2*A_fenster2+U_fenster3*A_fenster3);
283
284 for j in 1:n loop
285     qs[j]=alphaw[j]*Sw[j]*I[j]; //solar gains exterior walls
286     qsg[j]=tau[j]*Swin[j]*I[j]; //solar irradiation through windows
287 end for;
288
289 algorithm
290     for j in 1:n_floor loop
291         qsgf[j]:=(Swf[j]/sum(Swf))*alphaf*sum(qsg);
292         //solar radiation on interior wall surface
293     end for;
294     for j in 1:n loop
295         qsgw[j]:=(Sw[j]/sum(Sw))*(1 - alphaf)*sum(qsg);
296         //solar radiation of floor
297     end for;
298
299
300 algorithm //for control of heating and cooling
301     if Ti<=295.15 and -L - Q_inf - Q_w - Q_win>0 then
302         HC:=-L - Q_inf - Q_w - Q_win;
303     elseif Ti<=295.15 and -L - Q_inf - Q_w - Q_win<=0 then
304         HC:=0;
305     elseif Ti>=299.15 and -L - Q_inf - Q_w - Q_win<0 then

```

```

306      HC:=-L - Q_inf - Q_w - Q_win;
307      elseif Ti>=299.15 and -L - Q_inf - Q_w - Q_win>=0 then
308        HC:=0;
309      else
310        HC:=0;
311      end if;
312
313      annotation (uses(Modelica(version="3.2.1")),
314        experiment(StopTime=3.15324e+007, Interval=3600),
315        __Dymola_experimentSetupOutput);
316 end offices2_detailed_convection_model;

```